Central role for melanocortin-4 receptors in offspring hypertension arising from maternal obesity

Anne-Maj S. Samuelsson[a,1], Amandine Mullier[a], Nuria Maicas[a], Nynke R. Oosterhuis[b], Sung Eun Bae[a], Tatiana V. Novoselova[c], Li F. Chan[c], Joaquim M. Pombo[a], Paul D. Taylor[a], Jaap A. Joles[b], Clive W. Coen[a], Nina Balthasar[d], and Lucilla Poston[a]

[a]Division of Women's Health, King's College London, Women's Health Academic Centre King's Health Partners, London SE1 7EH, United Kingdom; [b]Department of Nephrology and Hypertension, University Medical Center Utrecht, Utrecht 3584 CX, The Netherlands; [c]William Harvey Research Institute, Barts and the London School of Medicine, Queen Mary University of London, London EC1M, United Kingdom; and [d]School of Physiology and Pharmacology, University of Bristol, Bristol BS8 1TH, United Kingdom

Melanocortin-4 receptor (Mc4r)–expressing neurons in the autonomic nervous system, particularly in the paraventricular nucleus of the hypothalamus (PVH), play an essential role in blood pressure (BP) control. Mc4r-deficient (Mc4rKO) mice are severely obese but lack obesity-related hypertension; they also show a reduced pressor response to salt loading. We have previously reported that lean juvenile offspring born to diet-induced obese rats (OffOb) exhibit sympathetic-mediated hypertension, and we proposed a role for postnatally raised leptin in its etiology. Here, we test the hypothesis that neonatal hyperleptinemia due to maternal obesity induces persistent changes in the central melanocortin system, thereby contributing to offspring hypertension. Working on the OffOb paradigm in both sexes and using transgenic technology to restore Mc4r in the PVH of Mc4rKO (Mc4rPVH) mice, we have now shown that these mice develop higher BP than Mc4rKO or WT mice. We have also found that experimental hyperleptinemia induced in the neonatal period in Mc4rPVH and WT mice, but not in the Mc4rKO mice, leads to heightened BP and severe renal dysfunction. Thus, Mc4r in the PVH appears to be required for early-life programming of hypertension arising from either maternal obesity or neonatal hyperleptinemia. Early-life exposure of the PVH to maternal obesity through postnatal elevation of leptin may have long-term consequences for cardiovascular health.

melanocortin-4 receptors | developmental programming | maternal obesity | hypertension | sympathetic nerve activity

The main focus of research into the central melanocortin system has been on melanocortin-4 receptor(s) (Mc4r) and their relation to energy homeostasis, with relatively few studies addressing the role of Mc4r in cardiovascular control (1, 2). However, it is clear that this system plays an important role in the control of blood pressure (BP) (3, 4). In humans with loss-of-function Mc4r mutation, there is severe obesity but no obesity-related hypertension (5). Mc4r-deficient (Mc4rKO) mice exhibit hyperphagia and marked obesity and, similarly, no obesity-related hypertension (3). Mc4r deletion also reduces the pressor response to salt loading, as well as preventing inflammatory and renal damage associated with obesity (6). Pharmacological inhibition of Mc4r in adult rats reduces the obesity-related hypertension and renal sympathetic nerve activity (RSNA) associated with hyperleptinemia (7, 8). Moreover, the highest expression of hypothalamic Mc4r mRNA is found in the paraventricular nucleus of the hypothalamus (PVH), which integrates and responds to a variety of neural and humoral signals regulating RSNA (9–12). It has been shown that leptin stimulates the tonic firing rate of Mc4r PVH neurons in rats, resulting in heightened arterial pressure, a finding that is consistent with causal links between obesity and adult hypertension (13).

The increased prevalence of hypertension among children and young adults has been attributed to sympathetic hyperactivity (14). Although genetic and lifestyle factors undoubtedly contribute to raised BP in young people, hypertension may, at least in part, have origins in fetal and neonatal life (15, 16). In population studies, maternal obesity has been independently linked to adult offspring cardiovascular morbidity and mortality (17). We have previously demonstrated offspring juvenile hypertension in rats, independent of adiposity, resulting from prenatal exposure to maternal diet-induced obesity. This hypertension was associated with a shift in the sympathetic to parasympathetic ratio of heart rate variability (HRV), indicative of heightened sympathetic efferent tone (18, 19), persisting to adulthood (19, 20). These findings, together with the increase in renal norepinephrine and tyrosine hydroxylase (TH) expression (19), led us to propose that increased RSNA contributes to offspring cardiovascular dysfunction secondary to maternal obesity (18).

Previously, we suggested that overexposure to leptin in neonatal rats as a result of maternal obesity leads to hypertension through aberrant development of hypothalamic neuronal networks involved in BP homeostasis (18, 21); this hypothesis is consistent with several reports identifying neonatal leptin as an important neurotrophic factor during periods of early development (22, 23). Here, we address the hypothesis that maternal obesity-related leptin exposure in rodents in early life leads, through changes in the PVH melanocortin system, to chronically increased RSNA, hypertension, and renal dysfunction. Such a process may contribute to primary hypertension in an increasingly obese global human population.

Significance

Obesity is increasing in pregnant women worldwide. Independent associations have been reported between maternal obesity and metabolic cardiorenal disorders in the offspring, including hypertension. In this study, using genetically modified mice, we have identified a role for the hypothalamic paraventricular nucleus (PVH) melanocortin system in the etiology of hypertension. We show that maternal obesity permanently resets the responsiveness of the central sympathetic nervous system via this pathway. We conclude that neonatal leptin exposure is the primary mediator, because exogenous neonatal leptin administration to pups of lean mice leads to the same phenotype mediated by PVH melanocortin-4 receptors. Thus, primary hypertension of sympathetic origin can result from early-life exposure to maternal obesity, and the melanocortin pathway presents a target for intervention.

The previous use of mice with global Mc4r deletion in which Mc4r was restored in the sympathetic preganglionic neurons in the brainstem using Cre-lox methodology has led to recognition of a role in obesity-associated hypertension for Mc4r in these locations (24). Using a similar approach, we have now addressed the specific role of Mc4r PVH in the hypertension arising from maternal obesity in the mouse. In parallel experiments, we have also addressed the role of Mc4r PVH in the hypertension associated with experimental neonatal hyperleptinemia. The rat has also been used as a model to demonstrate the role of the Mc3/4 pathway in diet-induced obesity-related hypertension (25). To explore the origins of juvenile hypertension further, we also carried out pharmacological studies in offspring of diet-induced obese rats (OffOb). To determine the consequences for renal function, we examined renal histology, the renin/angiotensin system, oxidative stress, and inflammation.

Results

Mc3/4r Antagonism Attenuates Juvenile Hypertension in Rats Without Changing HR.
Juvenile (30-d-old) Sprague–Dawley rat OffOb had raised mean arterial pressure (MAP) vs. offspring of control dams (OffCon) (Fig. 1 A–C), which occurred before development of increased body weight (BW) induced by hyperphagia (Fig. S1 A–D). Chronic intracerebroventricular (ICV) Mc3/4r antagonist (SHU9119) infusion lowered MAP in male and female offspring (Fig. 1 B and C), with a greater reduction in hypertensive OffOb vs. normotensive OffCon rats (Fig. 1 F and G). Heart rate (HR) was unaffected in both sexes (Fig. 1 D and E). Renal denervation in OffOb rats led to normalization of MAP, suggesting that hypertension in the OffOb involves RSNA (Fig. 1 H and I). MAP

was unaffected by vehicle treatment in any group (Fig. S2 A and B). We also assessed the action of the Mc3/4r agonist melanotan II (MTII) on cardiovascular responses in male littermates in adulthood (360 d) (Fig. S3A). The i.p. administration of MTII rapidly increased MAP, without any effect on HR (Fig. S3 B–E). These experiments supported a role for Mc3/4r in hypertension arising from maternal obesity. Data on food intake (FI) and BW in these rats are provided in Supporting Information (Figs. S1 and S3). SHU9119 infusion for 5 d increased BW and FI more in OffOb, compared with OffCon (Fig. S1 A–D). MTII challenge reduced weight gain and FI in both OffOb and OffCon, compared with vehicle (Fig. S3 F and G).

MAP in WT, Mc4rKO, and PVH of Mc4rKO Mice with Maternal Diet-Induced Obesity.
To examine the role of Mc4r in the PVH on MAP, we used genetically modified mice (Fig. 2 and Tables S1 and S2). As in the rat (Fig. 1 B and C), MAP was raised in adult male and female OffOb-WT mice (Fig. 3 A and D). Mc4rKO mice showed no effect on MAP associated with maternal diet-induced obesity. OffOb mice with Cre-lox–induced Mc4r restoration in the PVH of Mc4rKO (Mc4rPVH; Fig. 2) mice showed greater MAP compared with OffOb-WT mice ($P < 0.05$). There was no change in HR except in male Mc4rPVH mice, which showed increased HR in OffOb vs. OffCon (Fig. 3 B and E). These findings in OffOb-Mc4rPVH mice were associated with an enhanced low-frequency/high-frequency (LF/HF) ratio in HRV spectral analysis (Fig. 3 C and F), heightened MAP elevation in response to the Mc3/4r agonist MTII (Fig. 3 G–I), and Mc4r restoration in the PVH (Fig. 3 J and K). Linear growth curves, body composition, and energy expenditure (EE) in these mice are provided in Supporting Information (Fig. S4 A and B and Table S3). It is notable
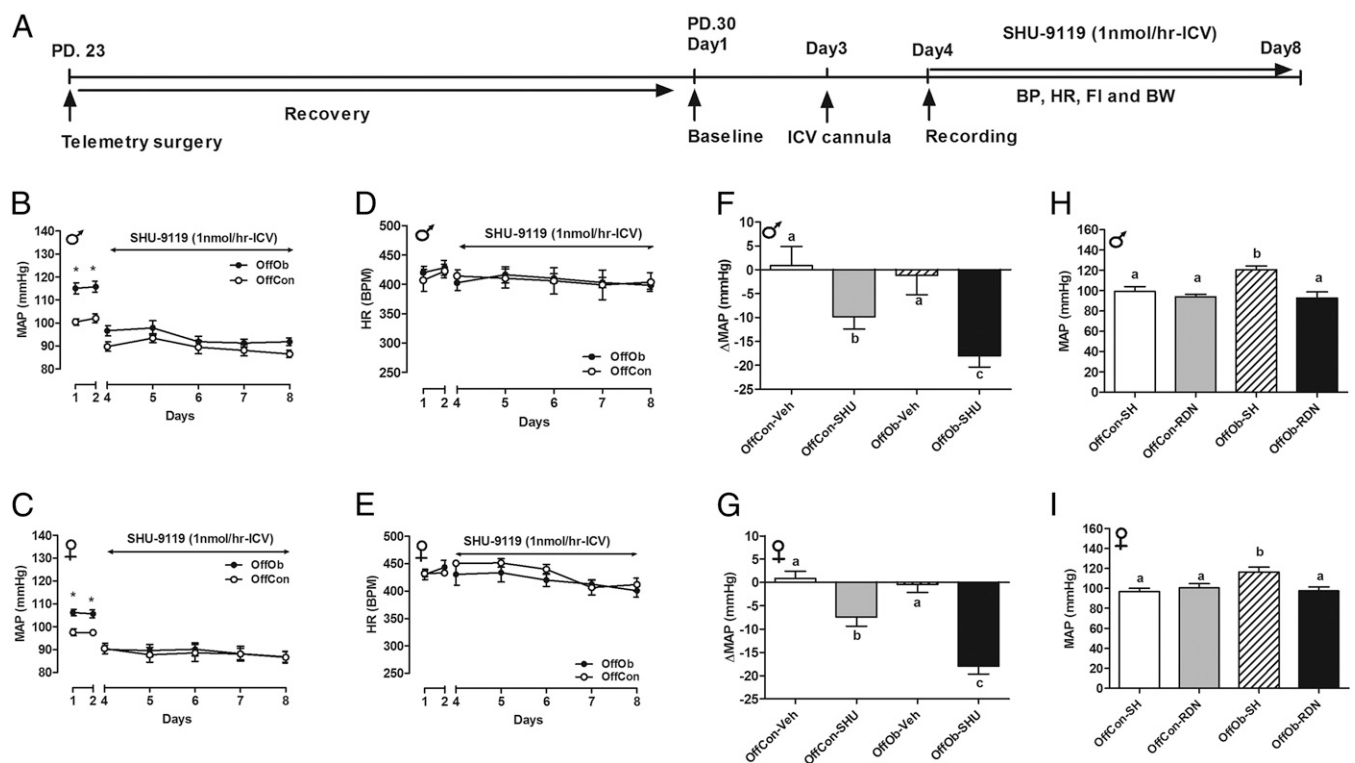

Fig. 1. Chronic Mc3/4r antagonist treatment in Sprague–Dawley rats (SHU-9119, 1 nmol·h^{-1}, ICV) attenuates juvenile hypertension, independent of heart rate (HR). Data in B–I were collected over 5 d (from day 33 to day 37) in OffOb and OffCon. (A) Mc3/4r antagonist (SHU-9119) or vehicle was infused for 5 d using an osmotic minipump. Mean arterial pressure (MAP) and HR responses were continuously monitored using radiotelemetry in male and female rats, respectively. MAP (B and C), HR (D and E), and changes in MAP (F and G) are shown. BPM, beats per minute. (H and I) Renal denervation (RDN) in OffOb rats normalized the MAP compared with sham-operated (SH) rats. Data are expressed as the daily average of MAP and HR per group ($n = 5$–6; mean $\pm$ SEM). *$P < 0.001$ vs. OffCon using the Student t test. Means not sharing the same letter are significantly different from each other ($P < 0.05$) by generalized least squares (GLS) regression analysis.
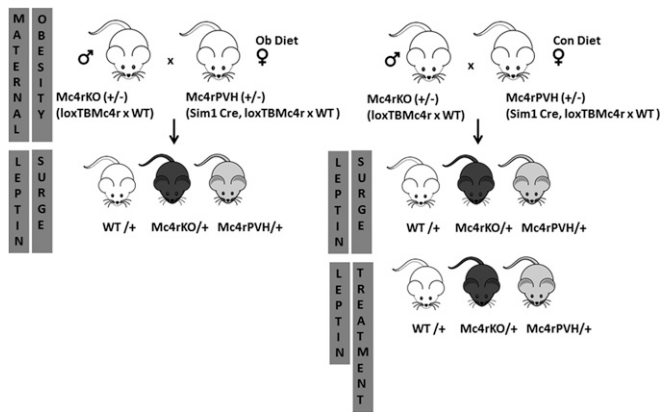
Fig. 2. Breeding and experimental protocol. Nontransgenic heterozygous Mc4rKO males (loxTBMc4r) were mated with transgenic heterozygous Mc4rPVH females (Sim1-Cre, loxTB Mc4r) to generate WT, homozygous Mc4rKO, and Mc4rPVH offspring. All mice are on a mixed C57Bl6/J, 129Sv, and FVB background. Littermates were used for all studies to avoid partial genetic background effects. In experimental protocol 1, dams were fed either a control diet (Con) or highly palatable obesogenic diet (Ob) 5 wk before mating and during pregnancy and lactation. OffCon- and OffOb-WT, -Mc4rKO, and -Mc4rPVH mice were weaned to a control diet at 21 d of age, genotyped, and then phenotyped at 6 mo of age. In experimental protocol 2, neonatal WT, Mc4rKO, and Mc4rPVH littermates born to obese (OffOb) or control (OffCon) dams were killed at PD6, PD9, and PD15 to trace the neonatal serum leptin surge. In experimental protocol 3, neonatal WT, Mc4rKO, and Mc4rPVH littermates were treated with leptin (NL, 3 mg/kg, twice daily, i.p.) or with vehicle (NS) on PD9–PD14. This neonatal hyperleptinemia protocol was designed to mimic the augmented and prolonged leptin surge found in the OffOb. More details are provided in *Supporting Information*.

that OffOb-WT and OffOb-Mc4rPVH (male) mice showed increased BW compared with OffCon-WT and OffCon-Mc4rPVH mice, respectively (Fig. S4). The reduced EE observed in the obese Mc4rKO mice was not rescued in Mc4rPVH mice (Table S3), indicating that PVH Mc4r are not involved in mediating the effects of melanocortins on EE.

Neonatal Leptin Profile in WT, Mc4rKO, and Mc4rPVH Mice. Given that our previous findings in rats implicated an augmented postnatal leptin surge in the etiology of hypertension and obesity in OffOb (18, 21), we next addressed possible links between postnatal leptin and Mc4r in relation to hypertension in male and female OffOb mice. All groups showed a postnatal serum leptin surge (Fig. 4 *A–C*, sexes combined): The concentrations were higher at postnatal day (PD) 9 and PD15 in OffOb-WT vs. OffCon-WT and in OffOb-Mc4rPVH vs. OffCon-Mc4rPVH (Fig. 4 *A* and *C*), with OffOb-Mc4rPVH showing an advanced elevation by PD6 (Fig. 4*C*). However, on PD9 and PD15, the elevated leptin concentrations in OffOb- and OffCon-Mc4rKO showed no additional influence of maternal diet-induced obesity (Fig. 4*B*). In all groups, the changes in neonatal leptin from PD6–PD15 (Fig. 4 *D–F*) did not correspond to the changes in neonatal BW, a finding that is consistent with the previous report that leptin does not influence energy balance in neonatal mice (26).

Effects of Neonatal Leptin Treatment on MAP in WT, Mc4rKO, and Mc4rPVH Mice. To assess the importance of neonatal hyperleptinemia in the onset of hypertension arising from maternal diet-induced obesity, WT, Mc4rKO, and Mc4rPVH mice born to control dams were treated twice daily with i.p. leptin on PD9–PD14 to mimic the neonatal leptin surge in OffOb mice (Fig. 2). In each genotype, this treatment resulted in metabolic profiles (Table S4) and BP profiles (Fig. S5 *A* and *D*) similar to the profiles found in the same genotype following exposure to maternal obesity, including absence

of hypertension in the neonatal leptin-treated (NL)-Mc4rKO mice (Fig. S5 *A* and *D*). These findings indicate that neonatal leptin exposure leads to hypertension in a process that is dependent on Mc4r. The similarities in MAP, HR, and HRV between the NL (Fig. S5 *A–F*) and OffOb (Fig. 3 *A–F*) mice strengthened the evidence for a causative role for neonatal hyperleptinemia in the hypertension that arises from maternal diet-induced obesity.

Effects of Acute Leptin Treatment in WT, Mc4rKO, and Mc4rPVH Mice. We have shown previously that juvenile OffOb rats lack the normal satiety response to leptin, despite maintenance of the pressor response (selective leptin sensitivity) (19). We therefore examined the acute effect of exogenous leptin in OffOb and OffCon mice (sexes combined) in WT, Mc4rKO, and Mc4rPVH genotypes to assess the role of Mc4r in selective leptin resistance. Leptin increased MAP in all groups except OffOb-Mc4rKO and OffCon-Mc4rKO mice (Fig. 5 *A–C*), with the highest pressor response being obtained in the OffOb-Mc4rPVH mice (Fig. 5*C*). Thus, the greater leptin-induced MAP elevation in OffOb mice seems to involve activation of Mc4r in the PVH. Leptin-induced suppression of appetite (Fig. 5*D*) and weight gain (Fig. 5*E*) were lost in the OffOb mice, thus demonstrating selective leptin sensitivity.

Development of Renal Dysfunction in WT and Mc4rPVH Mice with Neonatal Exposure to Leptin. Having implicated heightened sympathetic activation via Mc4r in the hypertension induced by either maternal obesity or experimental neonatal hyperleptinemia, we hypothesized that Mc4r deletion would protect against renal dysfunction associated with hypertension in the NL mice, and that Mc4rPVH restoration of Mc4r in the PVH would reverse this protection. This hypothesis was confirmed with an impaired glomerular filtration rate (GFR) in NL-WT and NL-Mc4rPVH male and female mice compared with respective neonatal saline-treated (NS) mice, whereas Mc4rKO male and female mice showed a similar GFR in NL vs. NS mice. Albuminuria, a marker of obesity-related renal injury, was elevated in all NL mice, with a threefold increase in the NL-Mc4rPVH mice, compared with NS-Mc4rPVH mice. Urinary markers of renal injury [neutrophil gelatinase-associated lipocalin (NGAL) and kidney injury molecule-1 (KIM-1)] were increased in NL-WT and NL-Mc4rPVH mice; Mc4rKO mice were protected against NL-induced renal injury. Fig. 6 shows data for these parameters in males; females were similar. Mc4rKO mice were also partly protected against renal injury. NL-WT and NL-Mc4rPVH male and female mice had enhanced cortical fibrogenesis, tubulointerstitial infiltration, and inflammation [cluster of differentiation 36 (CD36, macrophage scavenger)], compared with NL-Mc4rKO mice. Fig. S6 *A–F* shows these variables for males; females were similar. Renal injury was also associated with enhanced oxidative stress. Components of the reactive oxygen species were all increased accordingly to renal injury: thiobarbituric acid reactive substance(s) (TBARS; Fig. S7 *S* and *T*), NAPDH oxidase-4 (Nox-4) mRNA (Fig. S7 *Q* and *R*), and nitrotyrosine immunoreactivity (Fig. S6 *G* and *H*). These data provide further evidence for the importance of Mc4rPVH in the etiology of hypertension and renal disease resulting from exposure to maternal diet-induced obesity or experimental neonatal hyperleptinemia.

Mc4rKO mice also showed reduced RSNA and renin angiotensin system (RAS) as assessed by reduced mRNA expression for TH, renin, and angiotensin II receptor 1a (AT1a). Restoration of Mc4r in PVH neurons returned RSNA and RAS in Mc4rKO mice secondary to maternal obesity (Fig. S7 *A–F*) or neonatal hyperleptinemia (Fig. S7 *K–P*) to values similar to the values observed in the WT mice. Collectively, the data suggest that Mc4rPVH-mediated hypertension of sympathetic origin leads to renal injury.

Discussion

These experiments demonstrate (*i*) that functional Mc4r in the PVH are sufficient for early-life programming of hypertension of
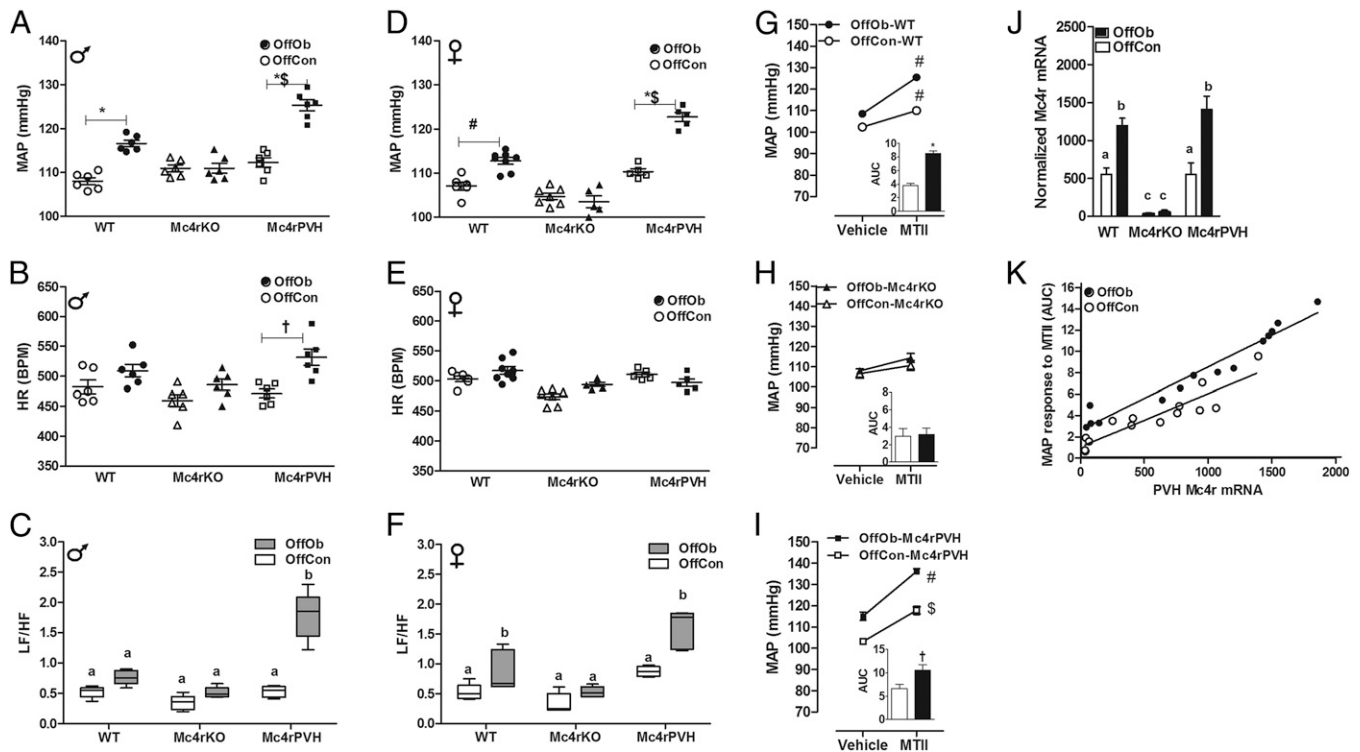
Fig. 3. Mc4r deletion (Mc4rKO) blunts the MAP in OffOb, whereas reactivation of Mc4r in the PVH completely rescued the increased MAP. Data in each panel were collected as average 24-h recordings from 6-mo-old male and female OffOb (black)- and OffCon (white)-WT, -Mc4rKO, and -Mc4rPVH mice. MAP (*A* and *D*), HR (*B* and *E*), and LF/HF ratio (*C* and *F*; LF, 0.04–0.15; HF, 0.15–0.40). *$P < 0.001$, †$P < 0.01$, and #$P < 0.05$ vs. OffCon; $$P < 0.05$ vs. OffOb-WT using the Student *t* test ($n = 6$–8 per group, mean ± SEM). (*G*–*I*) MAP responses to MTII challenge (Mc3/4r agonist, 10 mg/kg, i.p.). Responses are demonstrated as area under the curve (AUC). #$P < 0.001$ and $$P < 0.05$ vs. Vehicle; *$P < 0.001$ and †$P < 0.05$ vs. OffCon using the Student *t* test ($n = 6$–8 per group, sex combined, mean ± SEM). (*J*) Mc4r mRNA in laser-dissected PVH normalized to the housekeeping genes β-actin and RPL13A (using the GeNorm program; $n = 4$–6 per group, sex combined). Means not sharing the same letter are significantly different from each other ($P < 0.05$) by generalized least squares (GLS) regression analysis. (*K*) α-MSH sensitivity curve with MAP response to MTII (*y* axis) vs. PVH Mc4r mRNA expression (*x* axis) in 6-mo-old OffCon (white)- vs. OffOb (black)-WT, -Mc4rKO, and -Mc4rPVH mice. OffOb showed a higher slope ($P < 0.05$) in the α-MSH sensitivity curve vs. OffCon [analysis of covariance (ANCOVA), $n = 13$].

sympathetic origin arising from maternal obesity, (*ii*) that neonatal hyperleptinemia is a likely mediator, and (*iii*) that the hypertension is associated with deterioration of kidney function. The adult phenotype identified in the mice studied here bears a striking resemblance to human hypertension of sympathetic origin (27).

Reversal of the hypertension by Mc3/4r antagonism (SHU-9119) in young, lean OffOb rats suggests that early-onset primary hypertension, independent of BW, is mediated by the melanocortin system activating the renal sympathetic system. Use of this antagonist cannot distinguish between Mc3r or Mc4r effects, or identify the anatomical location of the responsible receptors. We therefore sought to refine our investigative method. Because Mc4r is highly expressed in parvocellular neurons of the PVH (28), in a subset of neurons that control renal sympathetic tone (29, 30), we focused on Mc4rPVH mice. Using genetically modified mice in which Mc4r had been either completely deleted (Mc4rKO) or reinstated locally in the PVH (Mc4rPVH) (31), we found that the presence of Mc4r in the PVH was sufficient to restore early-life programming of raised BP. These results suggest a pivotal role for MC4r in the PVH; they do not detract from the reported BP effects of Mc4r at other sites, such as the nucleus tractus solitaries (32).

The increased LF/HF ratio in HR spectral analysis in OffOb-WT and OffOb-Mc4rPVH mice provided confirmation of sympathetic hyperactivity. In contrast, OffOb- and OffCon-Mc4rKO mice remained normotensive with evidence of both parasympathetic excitation and sympathosuppression. The higher BP in OffOb-Mc4rPVH mice than in OffOb-WT mice may indicate that Mc4r activation at other central locations (e.g., within the hypothalamus or brainstem) antagonizes Mc4r-mediated cardiovascular control

pathways from the PVH. An alternative explanation could be development of Mc4r hypersensitivity in the Mc4rPVH mice in response to neonatal hyperleptinemia. Restoration of Mc4r in the PVH completely rescued the increased BP observed in WT mice arising from maternal diet-induced obesity.

The independence of the heightened arterial pressure from the HR in the OffOb-Mc4rPVH mice strongly suggests that Mc4r in the PVH regulates sympathetic innervation in the kidney, but not in the heart, consistent with the rat model of dietary-induced obesity in which Mc3/4r antagonism reduced arterial pressure more in high-fat–fed compared with normal-fat–fed rats, independent of HR (25). We conclude that maternal obesity leads to increased juvenile offspring renal sympathetic tone and BP, which is offset by vagal-mediated adjustments in HR.

Strikingly similar phenotypes were obtained in offspring exposed to maternal diet-induced obesity or to experimental neonatal hyperleptinemia (mimicking the augmented leptin surge seen in the former group). Both experimental models resulted in elevated BP and greater BP responsiveness to exogenous leptin in adulthood. The postnatal leptin surge has been shown to have neurotrophic effects in the developing brain (23) and to influence plasticity of the melanocortin system (33). We have previously demonstrated in rats that neonatal hyperleptinemia associated with maternal obesity leads to juvenile hypertension and cardiac dysfunction (18, 21). The present results in mice with an experimentally enhanced leptin surge point to a role for maternal obesity-related neonatal hyperleptinemia in the restored PVH Mc4r expression and the onset of hypertension. Whether this increase in receptor expression within the PVH is associated with an increased local availability of
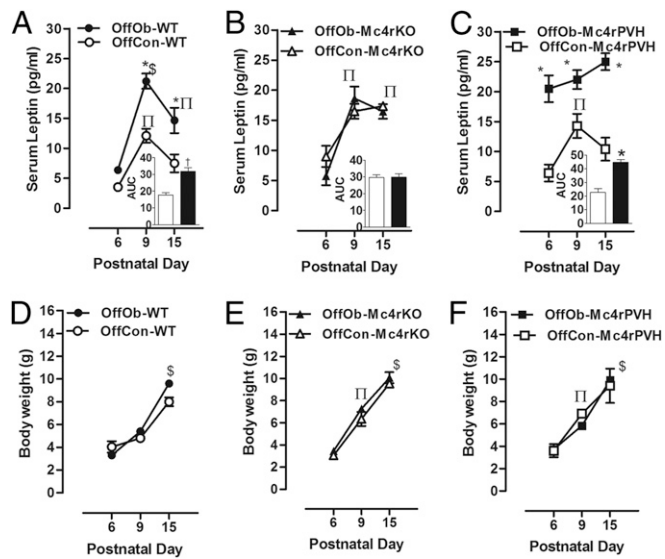
NEUROSCIENCE

Fig. 4. Neonatal leptin surge (at PD6, PD9, and PD15) was augmented and prolonged in WT and Mc4rPVH OffOb mice vs. WT and Mc4rPVH mice born to lean dams (OffCon). The neonatal serum leptin (*A–C*) and BW (*D–F*) were recorded at PD6, PD9, and PD15. Data are presented as AUC from baseline (*n* = 6–8 per group, sex combined). Data are expressed as mean ± SEM. *$P <$ 0.001 and †$P <$ 0.01 vs. OffCon using the Student *t* test; $^{$}P <$ 0.001 and $^{\Pi}P <$ 0.05 vs. PD6 using the Student *t* test.

α-melanocyte-stimulating hormone (α-MSH) is unknown. A previous study found no changes in α-MSH-immunoreactivity projections from the arcuate nucleus to the preautonomic division of the PVH in leptin-null mice with or without postnatal leptin replacement (22). However, the experimental model used in the present study involved leptin in excess rather than as a replacement for deficiency.

Leptin-induced sympathetic overactivity is a well-established phenotype for obesity-related hypertension (8) and is mediated by Mc4r (3). Our study confirms that acute pressor responses to leptin require functional Mc4r; it also makes the observation that these responses require Mc4r in the PVH. Our hypothesis that the pressor response would be higher than normal in OffOb or NL animals was confirmed. We conclude that programmed changes in melanocortin receptor expression are responsible for the heightened pressor responsiveness to exogenous leptin. Should these mouse models be translatable to the human condition, it may be expected that prenatal exposure to maternal obesity would result in an exaggerated pressor response to endogenous leptin.

The present study has confirmed that OffOb develop hypertension due to sympathetic overactivity. We pursued the hypothesis that maternal obesity could lead to offspring hypertension and renal dysfunction. The discovery of increased renal renin, AT1a, and TH expression further emphasizes the RSNA origins of the hypertension. Markers of oxidative stress (TBARS, Nox-4, and nitrotyrosine) and of leukocyte infiltration suggest pathways leading to renal injury, as evidenced by fibrosis, reduced GFR, and increased albumin, NGAL, and KIM-1 excretion. All of these observations were paralleled in the NL mice. Protection against neonatal leptin-induced renal injury in the Mc4rKO mice establishes a necessary role for this receptor. Thus, Mc4rKO mice were protected not only against maternal obesity-related hypertension but also against the associated maternal obesity-related renal injury. Despite being obese and hyperphagic, with prolonged exposure to metabolic disturbances, including hyperinsulinemia and hyperleptinemia, Mc4rKO OffOb or Mc4rKO NL mice showed no signs of hypertension or renal injury.
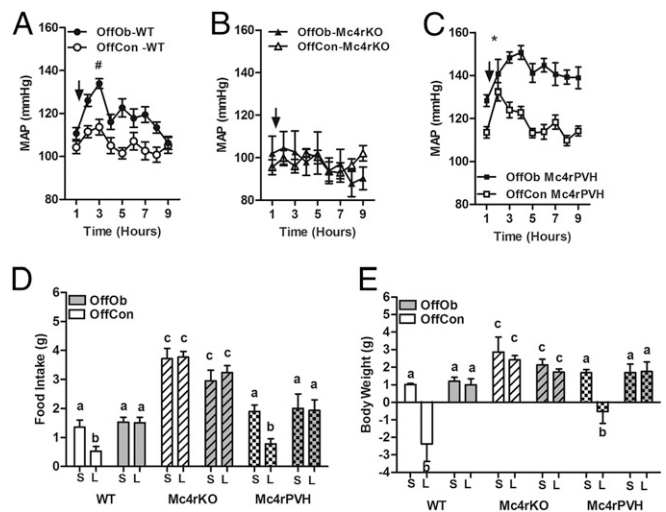

Fig. 5. Selective leptin sensitivity arising from maternal diet-induced obesity is mediated via Mc4r PVH. Mice (6 mo) were injected with saline (S, vehicle) or leptin (L, 10 mg/kg, i.p.) after an overnight fast in OffOb- and OffCon-WT, -Mc4rKO, and -Mc4rPVH mice, and FI and BP (MAP) were monitored. (*A–C*) MAP after leptin challenge in OffOb- vs. OffCon-WT, -Mc4rKO, and -Mc4rPVH mice. MAP returned to baseline (1) in all mice except OffOb-Mc4rPVH. Mc4rKO mice showed no pressor response to leptin. FI (*D*) and weight gain (*E*) after an overnight fast in OffOb-WT Mc4rKO and Mc4rPVH offspring are compared with respective controls. Mc4rKO mice were insensitive to the effect of leptin and failed to reduce FI and BW. Data are expressed as mean ± SEM (*n* = 6–8 per group, sexes combined). *$P <$ 0.001 and #$P <$ 0.05 vs. OffCon using the Student *t* test. Means not sharing the same letter are significantly different from each other (*P* < 0.05) by generalized least squares (GLS) regression analysis.

Increases in the prevalence of chronic kidney disease in childhood have paralleled the rise in overweight and obesity in children. Although the mechanisms responsible for obesity-induced chronic kidney disease are not fully understood, there is considerable evidence that abnormal sympathetic activation plays a key role (34), but this abnormal sympathetic activation has been generally attributed directly to obesity. The present study indicates origins of sympathetic overactivity in young adults that are
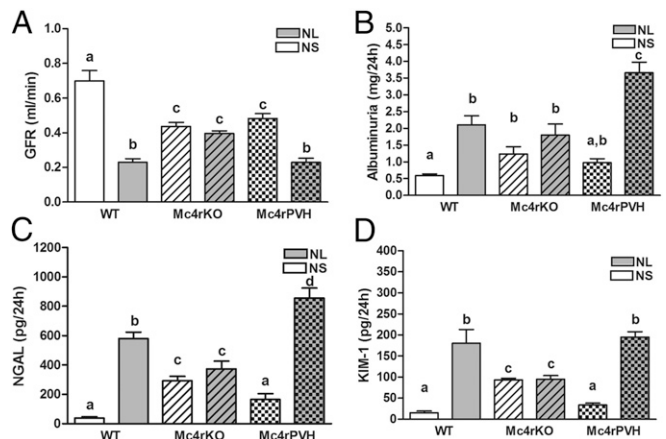
Fig. 6. Evidence of kidney dysfunction and injury in NL male mice. Mc4rKO mice are protected against neonatal leptin-induced renal injury. GFR (*A*, milliliters per minute), excretion of albumin (*B*, milligrams per 24 h), and the early renal damage markers NGAL (*C*, picograms per 24 h) and KIM-1 (*D*, picograms per 24 h) are shown. Data are expressed as mean ± SEM (*n* = 5–6 per group). Means not sharing the same letter are significantly different from each other (*P* < 0.05) by generalized least squares (GLS) regression analysis. Data for females were similar.

independent of obesity; it identifies a specific hypothalamic region and receptor system involved in early programming of hypertension and kidney disease induced by maternal obesity or experimental neonatal hyperleptinemia.

Materials and Methods

Experimental details are provided in *Supporting Information*.

Animals. All experiments were approved by the Local Ethics Committee of the University of King's College London and were conducted according to the Home Office Animals (Scientific Procedures) Act of 1986 (United Kingdom). Sprague–Dawley rats were bred and maintained as described previously (18) and treated with the Mc3/4r antagonist (SHU-9119, 1 nmol, ICV) or the Mc3/4r agonist MTII (2 mg/kg, i.p.).

Mc4rKO (loxTB MC4R) and Mc4rPVH (Sim1-Cre, loxTB MC4R) mice were generated as previously described (31). Sim1-Cre genetically modified mice were crossed with homozygous loxTB MC4R mice to obtain homozygous Sim1-Cre, loxTB MC4R mice. Nongenetically modified heterozygous loxTBMC4R and heterozygous Sim1-Cre, loxTB MC4R mice were used in the different experimental protocol (Fig. 2). To investigate the effect of in utero and early postnatal exposure to maternal obesity in all three offspring genotypes (WT, Mc4rKO, and Mc4rPVH), the dams were fed either a highly palatable energy-rich obesogenic diet or a control standard laboratory chow diet 5 wk before mating and throughout pregnancy and lactation, as described previously (20). The highly palatable diet consists of 20% animal lard, 10% simple sugars, 28% polysaccharide, and 23% protein (wt/wt) and energy of 4.5 kcal/g (Special Dietary Services, Wittam, U.K.), supplemented with sweetened condensed milk [∼55% simple sugars and 8% fat (wt/wt); Nestlé], which was fortified with 3.5% mineral mix and 1% vitamin mix (wt/wt) (AIN 93G; Special Diets Services). To validate the genetically modified mice, ear punch samples were collected for genotyping using three primers: (*i*) 5′GCAGTACAGCGAGTCTCAGG3′, (*ii*) 5′GTGCAAGTGCAGGTGCCAG3′, and (*iii*) 5′CTCCAACAGGCTTATGACACC3′.

Primers *ii* and *iii* detect the loxP-modified allele, whereas primers 1and 3 detect an endogenous genomic Mc4r fragment. A detailed description is provided in *Supporting Information*. At 6 mo of age, BP monitoring was conducted using mouse transmitters (TA11PA-C10; Data Science International, Inc.). After 1 wk of recovery, continuous data collection was monitored using the Dataquest A.R.T. Acquisition System (LabPRO Acquisition System version 3.01; Data Science International, Inc.). All hemodynamic data were analyzed using hourly means. To determine the influence of maternal obesity and neonatal hyperleptinemia on pressor and satiety responses to exogenous leptin in adulthood, as well as the role of the Mc4r, a leptin challenge (10 mg/kg, i.p.) was performed after an overnight fast as described (18) in male and female 6-mo-old mice. FI was measured by indirect calorimetry using the Comprehensive Laboratory Animal Monitoring System (TSE). To assess renal function, mice were fasted with ad libitum access to sugar water (1%); 24-h urine samples were measured and collected; and serum samples were analyzed to examine renal hemodynamics and renal injury markers. Tissues were harvested immediately, with the left kidneys being placed in formalin for fixation and later histological analysis, whereas the right kidneys were snap-frozen in liquid nitrogen. Details are provided in *Supporting Information*.

Statistical Analysis. Data are expressed as mean ± SEM. The effects of diet, genotype, and sex were investigated by random effects generalized least squares regression, grouping by dam, with robust variance estimates (35). Cardiovascular analysis was performed by the Student *t* test or one-way ANOVA for repeated measurements, followed by the Tukey post hoc test. Analysis was carried out using the statistical package Stata version 14 (StataCorp) or Prism 6 (GraphPad Software, Inc.).

1. Krashes MJ, Lowell BB, Garfield AS (2016) Melanocortin-4 receptor-regulated energy homeostasis. *Nat Neurosci* 19(2):206–219.
2. Samuelsson AM (2014) New perspectives on the origin of hypertension; the role of the hypothalamic melanocortin system. *Exp Physiol* 99(9):1110–1115.
3. da Silva AA, do Carmo JM, Wang Z, Hall JE (2014) The brain melanocortin system, sympathetic control, and obesity hypertension. *Physiology (Bethesda)* 29(3):196–202.
4. Li P, et al. (2013) Melanocortin 3/4 receptors in paraventricular nucleus modulate sympathetic outflow and blood pressure. *Exp Physiol* 98(2):435–443.
5. Greenfield JR (2011) Melanocortin signalling and the regulation of blood pressure in human obesity. *J Neuroendocrinol* 23(2):186–193.
6. do Carmo JM, et al. (2009) Impact of obesity on renal structure and function in the presence and absence of hypertension: Evidence from melanocortin-4 receptor-deficient mice. *Am J Physiol Regul Integr Comp Physiol* 297(3):R803–R812.
7. da Silva AA, Kuo JJ, Hall JE (2004) Role of hypothalamic melanocortin 3/4-receptors in mediating chronic cardiovascular, renal, and metabolic actions of leptin. *Hypertension* 43(6):1312–1317.
8. Haynes WG, Morgan DA, Djalali A, Sivitz WI, Mark AL (1999) Interactions between the melanocortin system and leptin in control of sympathetic nerve traffic. *Hypertension* 33(1 Pt 2):542–547.
9. Gabor A, Leenen FH (2012) Central neuromodulatory pathways regulating sympathetic activity in hypertension. *J Appl Physiol (1985)* 113(8):1294–1303.
10. Rahmouni K, Haynes WG, Morgan DA, Mark AL (2003) Role of melanocortin-4 receptors in mediating renal sympathoactivation to leptin and insulin. *J Neurosci* 23(14):5998–6004.
11. Cone RD (2005) Anatomy and regulation of the central melanocortin system. *Nat Neurosci* 8(5):571–578.
12. Li P, et al. (2013) Melanocortin 4 receptors in the paraventricular nucleus modulate the adipose afferent reflex in rat. *PLoS One* 8(11):e80295.
13. Schneeberger M, Gomis R, Claret M (2014) Hypothalamic and brainstem neuronal circuits controlling homeostatic energy balance. *J Endocrinol* 220(2):T25–T46.
14. Sorof J, Daniels S (2002) Obesity hypertension in children: A problem of epidemic proportions. *Hypertension* 40(4):441–447.
15. Luyckx VA, et al. (2013) Effect of fetal and child health on kidney development and long-term risk of hypertension and kidney disease. *Lancet* 382(9888):273–283.
16. Filler G, et al. (2011) Big mother or small baby: Which predicts hypertension? *J Clin Hypertens (Greenwich)* 13(1):35–41.
17. Reynolds RM, et al. (2013) Maternal obesity during pregnancy and premature mortality from cardiovascular event in adult offspring: follow-up of 1 323 275 person years. *BMJ* 347:f4539.
18. Samuelsson AM, et al. (2013) Experimental hyperleptinemia in neonatal rats leads to selective leptin responsiveness, hypertension, and altered myocardial function. *Hypertension* 62(3):627–633.
19. Samuelsson AM, et al. (2010) Evidence for sympathetic origins of hypertension in juvenile offspring of obese rats. *Hypertension* 55(1):76–82.
20. Samuelsson AM, et al. (2008) Diet-induced obesity in female mice leads to offspring hyperphagia, adiposity, hypertension, and insulin resistance: a novel murine model of developmental programming. *Hypertension* 51(2):383–392.
21. Kirk SL, et al. (2009) Maternal obesity induced by diet in rats permanently influences central processes regulating food intake in offspring. *PLoS One* 4(6):e5870.
22. Bouyer K, Simerly RB (2013) Neonatal leptin exposure specifies innervation of presympathetic hypothalamic neurons and improves the metabolic status of leptin-deficient mice. *J Neurosci* 33(2):840–851.
23. Bouret SG, Draper SJ, Simerly RB (2004) Trophic action of leptin on hypothalamic neurons that regulate feeding. *Science* 304(5667):108–110.
24. Sohn JW, et al. (2013) Melanocortin 4 receptors reciprocally regulate sympathetic and parasympathetic preganglionic neurons. *Cell* 152(3):612–619.
25. Dubinion JH, da Silva AA, Hall JE (2010) Enhanced blood pressure and appetite responses to chronic central melanocortin-3/4 receptor blockade in dietary-induced obesity. *J Hypertens* 28(7):1466–1470.
26. Ahima RS, Prabakaran D, Flier JS (1998) Postnatal leptin surge and regulation of circadian rhythm of leptin by feeding. Implications for energy homeostasis and neuroendocrine function. *J Clin Invest* 101(5):1020–1027.
27. Hall JE, et al. (2010) Obesity-induced hypertension: role of sympathetic nervous system, leptin, and melanocortins. *J Biol Chem* 285(23):17271–17276.
28. Elmquist JK (2001) Hypothalamic pathways underlying the endocrine, autonomic, and behavioral effects of leptin. *Int J Obes Relat Metab Disord* 25(Suppl 5):S78–S82.
29. Coote JH (2005) A role for the paraventricular nucleus of the hypothalamus in the autonomic control of heart and kidney. *Exp Physiol* 90(2):169–173.
30. Ramchandra R, Barrett CJ, Guild SJ, Malpas SC (2006) Evidence of differential control of renal and lumbar sympathetic nerve activity in conscious rabbits. *Am J Physiol Regul Integr Comp Physiol* 290(3):R701–R708.
31. Balthasar N, et al. (2005) Divergence of melanocortin pathways in the control of food intake and energy expenditure. *Cell* 123(3):493–505.
32. Tai MH, et al. (2007) Role of nitric oxide in alpha-melanocyte-stimulating hormone-induced hypertension in the nucleus tractus solitarii of the spontaneously hypertensive rats. *J Pharmacol Exp Ther* 321(2):455–461.
33. Zeltser LM, Seeley RJ, Tschöp MH (2012) Synaptic plasticity in neuronal circuits regulating energy balance. *Nat Neurosci* 15(10):1336–1342.
34. Hadtstein C, Schaefer F (2008) Hypertension in children with chronic kidney disease: Pathophysiology and management. *Pediatr Nephrol* 23(3):363–371.
35. Stock JH, Watson MW (2008) Heteroskedasticity-robust standard errors for fixed effects panel data regression. *Econometrica* 76(1):155–174.
36. Paxinos G, Franklin K (2001) *The Mouse Brain in Stereotaxic Coordinates* (Academic, San Diego), 2nd Ed.
37. Paxinos G, Watson C (1998) *The Rat Brain in Stereotaxic Coordinates* (Academic, New York), 4th Ed.
38. Stewart T, Jung FF, Manning J, Vehaskari VM (2005) Kidney immune cell infiltration and oxidative stress contribute to prenatally programmed hypertension. *Kid Int* 68(5): 2180–2188.
39. Ilse Raats CJ, et al. (1998) Differential Expression of Agrin in Renal Basement Membranes As Revealed by Domain-specific Antibodies. *J Biol Chem* 273:17832–17838.

NEUROSCIENCE

Supporting Information

Samuelsson et al. 10.1073/pnas.1607464113

SI Materials and Methods

Animal Care. All studies were approved by the Local Ethics Committee of the University of King's College London and were conducted according to the Home Office Animals (Scientific Procedures) Act of 1986 (United Kingdom).

Chemicals. All chemicals were obtained from Sigma–Aldrich unless otherwise specified.

Rodent Models. The influence of maternal diet-induced obesity on offspring cardiovascular and metabolic function was investigated in rats and mice.

Rat. Female Sprague–Dawley rats (60 d of age, weighing 208 ± 3 g; Banting & Kingman) were maintained under controlled conditions (light from 0700 to 1900 hours, 21 ± 3 °C, 40–50% humidity) and fed either a highly palatable obesogenic diet or a standard breeding diet (n = 8 per group). The obesogenic diet provided 6 wk before mating and throughout pregnancy and lactation consisted of a semisynthetic energy-rich and highly palatable pelleted diet [20% animal lard, 10% simple sugars, 28% polysaccharide, and 23% protein (wt/wt); energy of 4.5 kcal/g; Special Dietary Services], supplemented with sweetened condensed milk [~55% simple sugars and 8% fat (wt/wt); Nestlé], which was fortified with 3.5% mineral mix and 1% vitamin mix (wt/wt) (AIN 93G; Special Dietary Services). The control rats received the standard maintenance diet (RM1; Special Diets Services) until 10 d before mating, when they were given the standard breeding diet [3% animal lard and 7% simple sugar (wt/wt), energy of 3.5 kcal/g, RM3; Special Dietary Services] until weaning, as described previously (19). Litter size was standardized to eight pups (four male and four female) 48 h after birth. All of the offspring were weaned at 21 d of age and subsequently fed a standard maintenance diet (RM1) ad libitum. One male and one female from each litter were submitted to stereotaxic surgery at 30 d of age for implantation of an ICV cannula and drug administration (discussed below), and cardiovascular and metabolic function was evaluated during drug treatment. At 1 y of age, a subset of rats (n = 12, male) were exposed to i.p. pharmacological interventions and cardiovascular function evaluated.

Generation of genetically modified OffOb mice. The main aim of this study was to dissect the central melanocortin pathway genetically and identify the roles of Mc4r in PVH in OffOb. The generation of homozygous Mc4rKO (loxTB Mc4r) and Mc4rPVH (Sim1-Cre, loxTB Mc4r in the PVH) mice and their genotypic and phenotypic characterization have been described by Balthasar et al. (31). Sim1-Cre genetically modified mice were crossed with homozygous loxTB Mc4r mice to obtain nongenetically modified heterozygous loxTBMc4r and heterozygous Sim1-Cre (Cre) mice for the breeding protocol (Fig. 2). Nongenetically modified heterozygous loxTB Mc4r offspring were mated with Sim1-Cre genetically modified heterozygous loxTB Mc4r littermates to generate WT, homozygous loxTB Mc4r (Mc4rKO), and Sim1-Cre, loxTB Mc4r (Mc4rPVH) offspring. The pregnant female mice were housed in groups of two to four mice and exposed to light from 0700 to 1900 hours at 21 ± 3 °C in 40–50% humidity. To investigate the effect of in utero and early postnatal exposure to maternal obesity in all three offspring genotypes (OffOb- and OffCon-WT, -Mc4rKO, and -Mc4rPVH), the dams were fed a highly palatable energy-rich obesogenic diet [20% animal lard, 10% simple sugars, 28% polysaccharide, and 23% protein (wt/wt); energy of 4.5 kcal/g; Special Dietary Services], supplemented with sweetened condensed milk [~55% simple sugars and 8% fat, (wt/wt); Nestlé], which was fortified with 3.5%

mineral mix and 1% vitamin mix (wt/wt) (AIN 93G; Special Diets Services), compared with control mice fed standard laboratory chow [3% fat and 7% simple sugar (wt/wt), energy of 3.5 kcal/g, RM3; Special Dietary Services] 5 wk before mating and throughout pregnancy and lactation, as described previously (20). OffOb and OffCon dams were weaned onto standard laboratory chow diet (energy of 3.3 kcal/g, RM1; Special Diets Services), and ear punch samples were collected for genotyping. Ear samples were stored in RNAlater (Ambion) and run with PCR assay using three primers (primer 1, 5′GCAGTACAGCGAGTCTCAGG3′; primer 2, 5′GT-GCAAGTGCAGGTGCCAG3′; and primer 3, 5′CTCCAACAG-GCTTATGACACC3′). Primers 2 and 3 detect the loxP-modified allele, whereas primers 1and 3 detect an endogenous genomic Mc4r fragment. All mice were on a mixed C57Bl6/J, 129Sv, and FVB background. Littermates were used for all studies to avoid genetic background effects.

Laser captures microdissection and RNA isolation. To validate the genetically modified mice, Mc4r mRNA expression in the PVH was determined using laser capture methodology. Coronal sections of 20-μm thickness were prepared on a cryostat and mounted on poly-L-lysine–coated glass slides. Sections were thawed and fixed for 30 s in 95% ethanol and then rehydrated (75% and 50% ethanol, 30 s each). After fixation, the slides were stained with 1% cresyl violet (1 min). The sections were then dehydrated in a graded ethanol series (50%, 75%, 95% and twice for 100%, 30 s each) and air-dried. All solutions were prepared with RNase-Free water (Ambion). Laser microdissection was performed using a P.A.L.M Microbeam Laser System (Zeiss). The hypothalamic PVH was microdissected, covering the region from plates 37–41 (bregma: −0.70 mm to −1.20 mm) as defined by Paxinos and Franklin (36). After each microdissection, captured cells were kept in RNAlater. Total RNA was isolated according to the manufacturer's protocol (RNAaqueous Micro Kit; Ambion). Quality of the total RNA samples was determined by electrophoresis, and quantity was determined using a NanoDrop spectrophotometer (NanoDrop Products). Quantitative PCR (QPCR; Thermal Cycler Corbett Rotorgene 6000 2-plex) for Mc4r PVH copy number was determined with cDNA standard curves using housekeeping genes (β-actin and RPL13A). To ensure specificity of the PVH dissection, within the laser capture material, we examined the expression of a number of genes expressed only in the neighboring hypothalamic nuclei. As negative controls, we used arcuate nucleus-specific AgRP, ventromedial nuclei-specific Sf-1, and lateral hypothalamus-specific melanin-concentrating hormone (MCH). As a positive control, we determined the expression of the gene encoding thyrotrophin-releasing hormone (TRH), which is highly expressed in the PVH.

The following primers were used:

Mouse Mc4r forward, 5′GCAGTACAGCGAGTCTCAGG-3′

Mouse Mc4r reverse, 5′-CTCCAACAGGCTTATGACACC-3′

Mouse AgRP forward, 5′-AATCTGTGAGCTGGGACTGC-3′

Mouse AgRP reverse, 5′-GCCTAATAAAGGGTCCACACG-3′

Mouse Sf1forward, 5′-CTGGGATATGGGGACTAGCA-3′

Mouse Sf1 reverse, 5′-CACCCCGACTCTTGGAAA-3′

Mouse MCH forward, 5′-ATTCAAAGAACACAGGCTC CAAAC-3′

Mouse MCH reverse, 5′-CGGATCCTTTCAG AGCAAGGTA-3′

Mouse TRH forward, 5′-GGTTTAGAGGAACTGCCGCTC-TG-3′

Mouse TRH reverse, 5′-GGCAGCCAACATAGCCATAGA-CCCA-3′

Mouse β-actin forward, 5′-CTAAGGCCAACCGTGAAAAG-3′

Mouse β-actin reverse, 5′-ACCAGAGGCATACAGGGACA-3′

Mouse RPL13A forward, 5′-ATCCCTCCACCCTATGACAA-3′

Mouse RPL13A reverse, 5′-GCCCCAGGTAAGCAAACTT-3′

Stereotaxic Surgery (Rat). To elucidate whether juvenile hypertension is mediated by central Mc4r, we infused ICV Mc4r antagonist in OffOb and recorded BP, before obesity. At 23 d of age, a radiotelemetry probe was surgically inserted into male obese ($n = 15$) and control ($n = 15$) Sprague–Dawley rats to measure BP by radiotelemetry (discussed below). One week after surgery, a stainless-steel cannula (26 gauge, 10 mm long) was implanted into the right lateral cerebral ventricle under isoflurane anesthesia using the following coordinates: anteroposterior, −0.5 mm from bregma; mediolateral, ±1 mm bregma; dorsoventral, −4.5 from bregma (37). The guide cannula was anchored into the place with screws and dental acrylic; the catheter was connected to an osmotic minipump (0.5 μL·h^{-1}, ICV; Alzet) for SHU-9119 (Mc3/4r antagonist, 1 nmol·h^{-1}) or to vehicle (saline) infusion for 7 d; and BW, FI, MAP, systolic blood pressure (SBP), diastolic blood pressure (DBP), and HR were recorded. After the experiment, the animals were culled and the brains were removed and sectioned to confirm the position of the cannula, using crystal violet. Rats with missed cannula placement were not included in the analysis.

Renal Nerve Ablation (Rat). To establish the influence of RSNA on BP, we conducted renal nerve ablation in littermates of rats used for the above SHU9119 experiment. Telemetered OffOb and OffCon 30-d-old Sprague–Dawley rats were subjected to bilateral renal denervation or sham surgery. Briefly, a midline dorsal lumbar incision was made bilaterally under general anesthesia (2% isoflurane in O_2 at 2 L·min^{-1}), and each kidney was exposed by retracting the abdominal muscles. Using a light microscope, the renal arteries were stripped of the surrounding nerve bundles and painted with 10% phenol in absolute ethanol to destroy any remnant nerves. After a 5-min exposure to the solution, the artery was washed with isotonic saline. In the sham group, the same approach was used, although nerves remained intact and were painted with saline. Renal denervation was confirmed by assessing whether the renal tissue content of norepinephrine was less than 10% of the mean value in the sham-operated group. Renal norepinephrine contents were determined in offspring using an enzyme immunoassay kit (ALPCO Diagnostics) according to the manufacturer's protocol.

BP Measurement by Radiotelemetry (Rat and Mouse). Rats and mice were anesthetized with 2% isoflurane in O_2 at 2 L·min^{-1} with pre- and postoperative analgesia (buprenorphine, 0.1 mg/kg).

In mice and juvenile rats, a vertical incision was made in the left axillary space and the right carotid artery was isolated using blunt dissection. The carotid artery was ligated with sutures (5-0 silk) at the site of bifurcation and 8–10 mm below, and it was retracted toward the head and tail to occlude the blood flow. The tip of the probe catheter was inserted into the carotid lumen using a needle as an introducer; the needle was then withdrawn, and the tip of the catheter was advanced to the point of obtaining a sinus signal using frequency modulation radio. The main body of the telemetry probe (TA11PA-C10; Data Science International, Inc.) was inserted s.c. and secured by suturing the skin. In adult rats, a routine laparotomy was performed; the

catheter was surgically implanted into the descending abdominal aorta, and the body of probe was transfixed to the abdominal wall (TA11PA-C40; Data Science International, Inc.). Following 1 wk of recovery, cardiovascular variables were routinely monitored and recorded by scheduled sampling for 10 s every 5 min (500-Hz sampling frequency) with A.R.T. (Dataquest IV; Data Science International, Inc.) software. HRV was analyzed from a 300-s continuous telemetric BP record made between 0900 and 1000 hours in undisturbed telemetered animals in a quiet room. Datasets recorded in a sinus rhythm with a 500-Hz sampling frequency were used. Time and frequency domain of HRV analysis was performed using an HRV module of Chart 5.0 analyzing software (ADInstruments). Spectral analysis quantified the LF/HF ratio between the LF (0.04–0.15 Hz) domain corresponding to parasympathetic and sympathetic innervations and the HF (0.15–0.40 Hz) domain corresponding to parasympathetic innervations.

Neonatal Leptin Profile (Mouse). We have previously shown an increased neonatal plasma leptin surge in offspring of WT obese rats compared with offspring of WT lean controls (21). To determine the influence of maternal obesity on the neonatal leptin surge in OffOb, we studied litters from diet-induced obese ($n = 22$) or lean ($n = 22$) heterozygous loxTB Mc4r dams and Sim1-Cre heterozygous loxTB Mc4r dams. Offspring were killed at PD6, PD9, and PD15 to determine the serum leptin profile in the neonatal mice offspring. At each time point, litters were killed by decapitation between 0800 and 1100 hours. BW was measured, blood samples were collected for serum leptin concentration using mouse Leptin ELISA (Chrystal Chem), and tail samples were collected for genotyping.

Exogenous Administration of Leptin in the Neonatal Period (Mouse). We investigated whether, as we previously reported in rats, exogenous administration of leptin in the neonatal period to mimic the exaggerated leptin surge in OffOb vs. OffCon rat offspring (21) (and also observed in all OffOb mice in the present study) was associated with elevated BP in adulthood, and whether Mc4r played a role. Neonatal male and female Con- WT, -Mc4rKO, and -Mc4rPVH mice were randomly selected for administration of leptin twice daily (NL, 3 mg/kg leptin, i.p.) at PD9–PD15 or treatment with saline (NS). All mice were weaned ad libitum onto standard laboratory chow. The cardiovascular and renal function was evaluated at 6 mo of age.

Leptin and MTII Challenges (Mouse). To determine the influence of maternal obesity and neonatal hyperleptinemia on pressor and satiety responses to exogenous leptin in adulthood, as well as the role of the Mc4r, a leptin challenge (10 mg/kg, i.p.) was performed after an overnight fast as described (18) in male and female 6-mo-old OffOb- and OffCon-WT, -Mc4rKO, and -Mc4rPVH mice and 6-mo-old NS- and NL-WT, -Mc4rKO, and -Mc4rPVH mice. FI was measured by indirect calorimetry using the Comprehensive Laboratory Animal Monitoring System (CLAMS; TSE). Mice were acclimatized in CLAMS cages for 2 d before experimental procedures. BP, FI, and weight responses to leptin were assessed by measuring the change in BW and FI during a 24-h period and the change in MAP 6 h after injection after overnight fasting. To examine the influences of maternal obesity on Mc4r and Mc3r regulation of BP, mice were injected with MTII (Mc3/4r agonist). Single-caged mice were injected i.p. with 10 mg/kg MTII in PBS at 1200 hours, their food was removed, and BP was recorded for the ensuing 3 h according to previous studies of oxygen consumption (31).

Renal Function Measurements. To address the influence of neonatal hyperleptinemia on the renal physiology, as well as the role of the Mc4r, renal function was assessed in 6-mo-old NS- and NL-Mc4rKO

and -Mc4rPVH mice. Mice were acclimatized for 2 d in metabolic cages with ad libitum access to food and water. On the day of experiment, mice were fasted with ad libitum access to sugar water (1%); 24-h urine samples were measured and collected, and serum samples were analyzed to examine renal hemodynamics. Serum and urine creatinine was measured by commercial kits (Enzymatic Assay; Chrystal Chem). GFR was measured as the creatinine clearance rate during 24 h. Urine albumin excretion was measured via an Albumin Mouse ELISA Kit (ab108792; Abcam). Kidney injury molecule (KIM)-1 excretion was measured by ELISA (RKM100; R&D Systems), and urine neutrophil gelatinase-associated lipocalin (NGAL) was measured in urine using a precoated ELISA (R&D Systems). To monitor lipid peroxidation, TBARS was measured in plasma using colormetric analysis (Cayman Chemicals). Tissues were harvested immediately, with the left kidneys placed in formalin for fixation and later histological analysis, whereas the right kidneys were snap-frozen in liquid nitrogen.

Renal RAS and Oxidative Stress Markers. Because sympathoexcitation leads to enhanced activation of the RAS, which is implicated in renal dysfunction, we measured cortical AT1a and renin mRNA expression by QPCR in 6-mo-old Ob- and Con-WT, -Mc4rKO, and -Mc4rPVH male and female mice and in 6-mo-old NS- and NL-WT, -Mc4rKO, and -Mc4rPVH male and female mice. Oxidative stress is another important risk factor that has been detected in early stages of kidney disease (15) and increases as the disease progresses (15). Reactive oxygen species are generated by several enzymes, including Nox-4. Cortical Nox-4 mRNA was performed using standard laboratory techniques in RNA extracted from the cortex from 6-mo-old mice. The profibrotic marker TGF-β1 is also associated with early-onset kidney dysfunction, and was therefore evaluated in the mouse kidney (6). Total RNA was extracted from the cortex of the right kidney of Ob and NL mice, compared with Con and NS mice, respectively, by the standard TRIzol (Sigma–Aldrich) method. RNA quantity and integrity were assessed by optical density (NanoDrop-1000 spectrophotometer; NanoDrop Products). Reverse transcription was carried out using a QuantiTect Reverse Transcriptase Kit (catalog no. 205311; Qiagen) according to the manufacturer's instructions; cDNA was stored at −80 °C. Intron-spanning primers for renin for real-time PCR were designed using the Universal Prolibrary (Roche Diagnostics Ltd. and Operon Biotechnologies GmbH). Amplification reactions were carried out (Thermal Cycler Corbett Rotorgene 6000 2-plex; Corbett Research), sample copy number was determined with cDNA standard curves using Rotorgene 6000 series software, and the GeNorm program was used to validate stable housekeeping genes (β-actin and TATABox). Cortical AT1a, renin, Nox-4, and TGF-β1 mRNA were expressed as a copy number/geometric mean of two housekeeping genes.

The following primers were used:

Mouse AT1a forward, 5′-ACTCACAGCAACCCTCCAAG-3′

Mouse AT1 reverse, 5′-CTCAGACACTGTTCAAAATGCAC -3′

Mouse TH forward, 5′-CCCAAGGGCTTCAGAAGAG-3′

Mouse TH reverse, 5′-GGGCATCCTCGATGAGACT-3′

Mouse renin forward, 5′-CCCGACATCTCCTTCAACC-3′

Mouse renin reverse, 5′-TGCACAGCTTGTCTCTCCTG -3′

Mouse Nox-4 forward, 5′-AAGTGGAGTAGCTTTCATTT-GGA-3′

Mouse Nox-4 reverse, 5′-GCTACAGTTTCAACCTCCCAGT-3′

Mouse TGF- β1 forward, 5′-CACCATCCATGACATGAACC-3′

Mouse TGF-β1 reverse, 5′-CCGCACACAGCAGTTCTTC-3′

Mouse β-actin forward, 5′-CTAAGGCCAACCGTGAAAAG-3′

Mouse β-actin reverse, 5′-ACCAGAGGCATACAGGGACA-3′

Mouse TATAbox forward, 5′-TCA CCA ATG ACT CCT ATG AC-3′

Mouse TATAbox reverse, 5′-GCC ACC TGT AAC TGA GTG-3′

Determination of Nitrotyrosine by Immunofluorescence. Renal oxidative stress has been associated with renal histopathology and was analyzed by renal nitrotyrosine (immunohistochemistry), which is common biomarker for oxidative stress (38). In brief, the frozen kidney tissue from 6-mo-old NS- and NL-WT, -Mc4rKO, and -Mc4rPVH mice was embedded Tissue-Tek Optimal Cutting Temperature compound. Serial tissue sections of 3 μm were cut, air-dried, and fixed in 2% paraformaldehyde (PFA) and 4% sucrose in PBS for 10 min. Sections were washed for 5 min in PBS and permeabilized by 0.3% Triton in PBS for 10 min. After washing, sections were blocked with blocking solution (2% FCS and 2% BSA in PBS) for 30 min. Samples were then incubated for 60 min at room temperature with the antinitrotyrosine primary antibody (Millipore) diluted in blocking solution. Sections were washed three times with PBS for 10 min and incubated with the Alexa Fluor 488-conjugated secondary antibody (Thermo Fisher Scientific) for 30 min at room temperature. After fixation with 1% PFA in PBS, sections were rinsed and mounted in Vectashield mounting medium. Nitrotyrosine staining was scored semiquantitatively on a scale from 0 to 5 based on the extent of positive immunofluorescence staining rated by an observer on blinded sections.

Kidney Histology. To elucidate whether renal oxidative stress was associated with structural changes, we assessed renal fibrogenesis and tubulointerstitial (TI) damage in 6-mo-old NS- and NL-WT, -Mc4rKO, and -Mc4rPVH mice. Formalin-fixed renal tissue (n = 4–8 per group) was dehydrated and subsequently embedded in paraffin. Kidneys were cut at different latitudes into 3-μm sections, mounted on Superfrost slides, and dried at 37 °C for at least 24 h. Sections were stained for 8 min with Weigert's hematoxylin and for 60 min with 0.1% Picro-Sirius Red for assessment of fibrotic tissue formation. Collagen fibers were colored bright red on a pale yellow background. On periodic acid–Schiff-stained sections TI damage was scored. In seven to 10 different nonoverlapping fields per animal, three variables for TI damage were scored on a scale of 1–5. Scored variables were the amount of peritubular inflammatory infiltrate, interstitial fibrosis, and tubular atrophy. All of the histopathological scores were performed on blinded sections.

Determination of Macrophages by Immunofluorescence. Sympathetic efferent nerves have been shown to play a key role in the regulation of peripheral and local inflammation and immune response (38). Frozen kidney tissue from 6-mo-old NS- and NL-WT, -Mc4rKO, and -Mc4rPVH mice was embedded in Tissue-Tek Optimal Cutting Temperature compound. Serial tissue sections of 3 μm were cut, air-dried, and fixed in acetone for 10 min at 4 °C. Sections were again air-dried and incubated for 45 min at room temperature with the corresponding primary antibodies diluted in PBS supplemented with 1% BSA/0.1% sodium azide (PBA): Double staining with a monoclonal antibody against the core protein of agrin (M191) (39), kindly provided by Johan van der Vlag (RUMC, Nijmegen, The Netherlands), and a monoclonal antibody against CD68 (AbDSerotec, Bio-Rad Laboratories, Inc.) was performed. Sections were washed three times with PBS for 10 min and incubated with the Alexa Fluor 488-conjugated secondary antibody (Invitrogen) and Cy3-conjugated secondary antibody (Jackson ImmunoResearch Laboratories) for 45 min at room temperature in PBA. After fixation with 1% PFA in PBS, sections were rinsed and mounted in Vectashield mounting medium. Macrophage staining was scored semiquantitatively on a scale from 0 to 5 based on the extent of CD68 immunofluorescence staining rated by an observer on blinded sections.

Statistical Analysis. Data are expressed as mean ± SEM. The effects of diet, genotype, and sex were investigated by random effects generalized least squares regression, grouped by dam, with robust variance estimates (35). Cardiovascular analysis was performed by the Student t test or one-way ANOVA for repeated measurements, followed by the Tukey post hoc test. Analysis was carried out using the statistical package Stata version 14 (StataCorp) or Prism 6 (GraphPad Software, Inc.).

Results

Female heterozygous Mc4r mice fed an obesogenic diet for 5 wk (ObMc4r$^{+/-}$) were ~50% heavier than control-fed heterozygous Mc4r mice (ConMc4r$^{+/-}$) before mating (Tables S1 and S2). Litter size and sex distribution were similar in all groups. In the WT and Mc4rPVH animals, adult BW of OffOb was higher than in OffCon,

and associated with increased FI, hyperinsulinemia, and hyperleptinemia (Table S3); because BW and FI did not differ between OffOb-Mc4rKO and OffCon-Mc4rKO mice, a key role for Mc4r in the metabolic phenotype of OffOb is indicated (Table S3). A further experiment investigated the importance of the neonatal leptin surge in the onset of hypertension: Con-WT, Con-Mc4rKO, and Con-Mc4rPVH mice were treated neonatally with leptin (Fig. 2) to mimic the augmented and prolonged leptin surge in OffOb mice (Fig. 4). This treatment in each genotype resulted in metabolic profiles (at 6 mo of age) markedly similar to the metabolic profiles in the same genotype following exposure to maternal obesity (Table S4), strengthening the evidence for a causative role for neonatal leptin in the metabolic phenotype in OffOb.
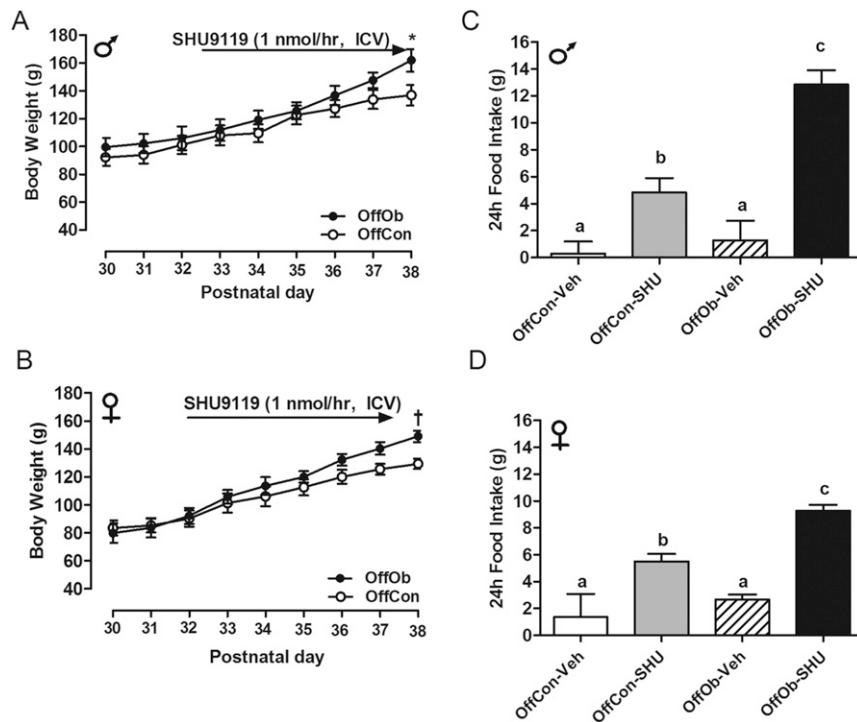

Fig. S1. SHU-9119 treatment in OffOb rats. ICV infusion of Mc3/4r antagonist [SHU9119 (1 nmol·h^{-1})] in juvenile (1-mo-old) male and female OffOb and OffCon rats. BW (*A* and *B*) and FI (*C* and *D*) are shown (*n* = 6). *$P < 0.001$ and †$P < 0.05$ vs. OffCon using the Student t test. Means not sharing the same letter are significantly different from each other ($P < 0.05$) by generalized least squares (GLS) regression analysis.
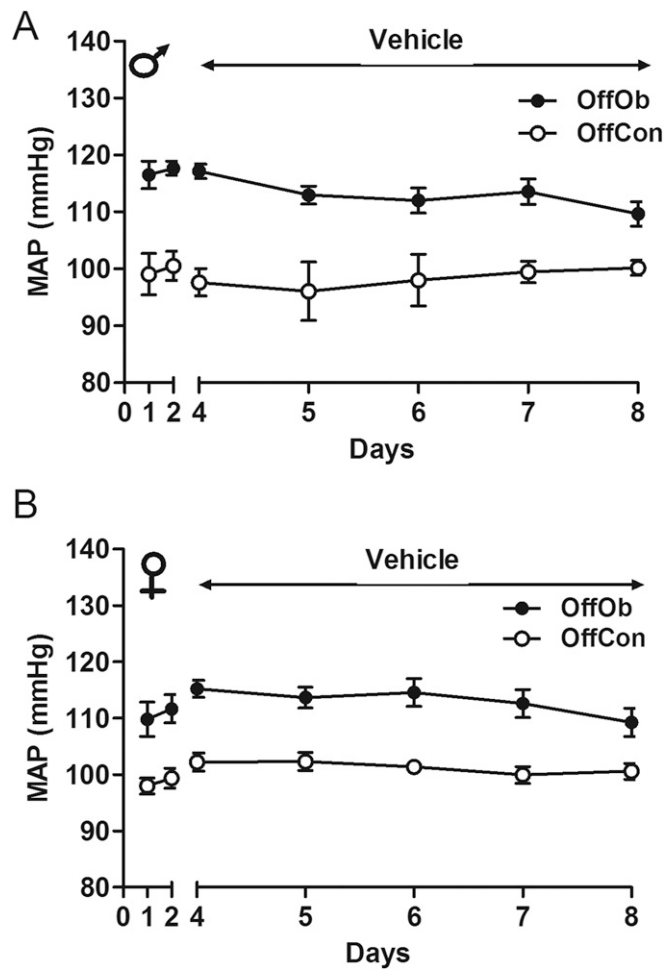
Fig. S2. MAP response to vehicle in OffOb rats. Mean arterial response to ICV infusion of vehicle in juvenile (1-mo-old) male (*A*) and female (*B*) OffOb rats compared with offspring of lean dams (OffCon) are shown. Data are shown as mean ± SEM (*n* = 6 per group).
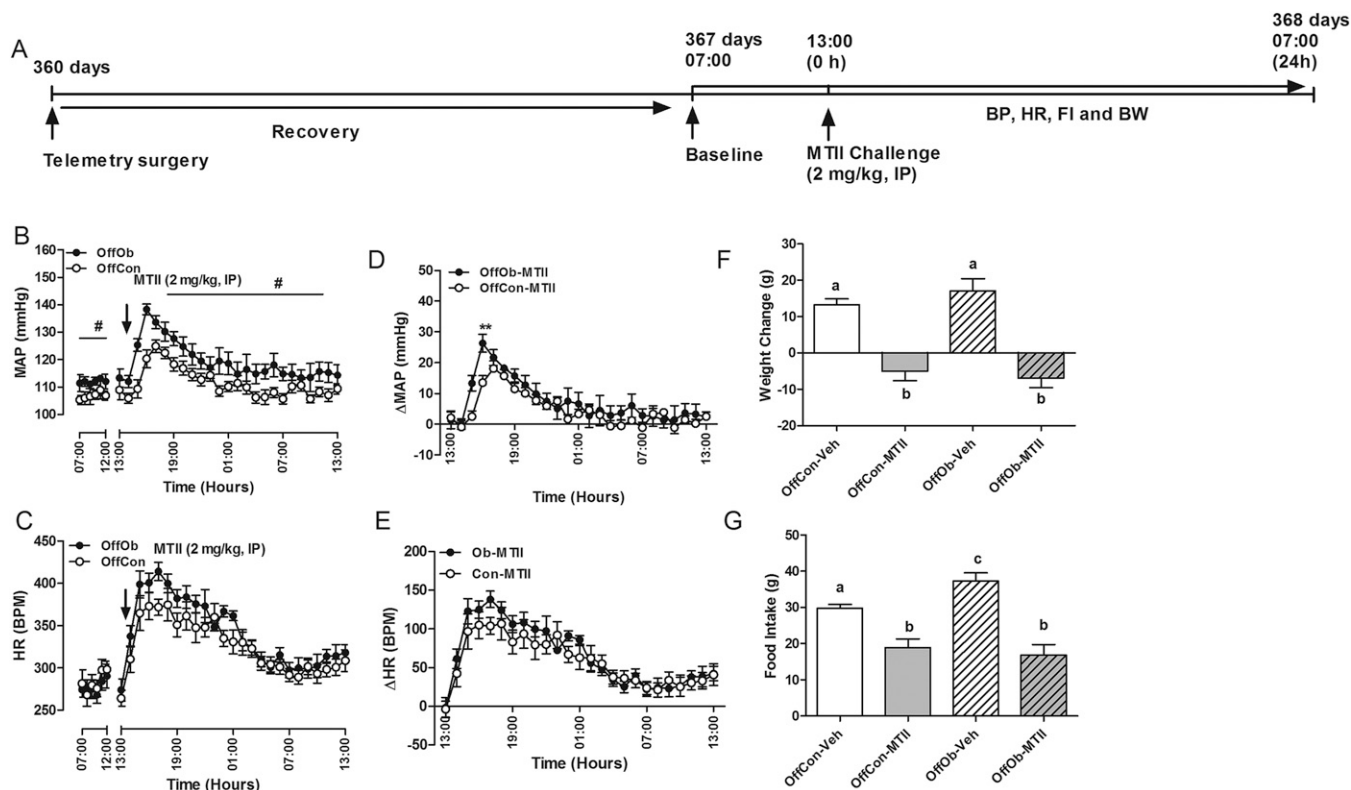
Fig. S3. (*A*) Injection (i.p.) of Mc3/4r agonist (MTII, 2 mg/kg) in adult (12-mo-old) male offspring at 1300 hours. MAP (*B* and *C*) and HR (*D* and *E*) responses to MTII change in BW (*F*) and FI (*G*) over the following 24 h are shown. BPM, beats per minute. Data are expressed as the hourly average of MAP and HR per group (*n* = 5–6; mean ± SEM). **$P < 0.01$ vs. OffCon using the Student *t* test. #$P < 0.001$, vs. OffCon, repeated measured ANOVA, followed by Tukey post hoc test. Means not sharing the same letter are significantly different from each other ($P < 0.05$) by generalized least squares (GLS) regression analysis.
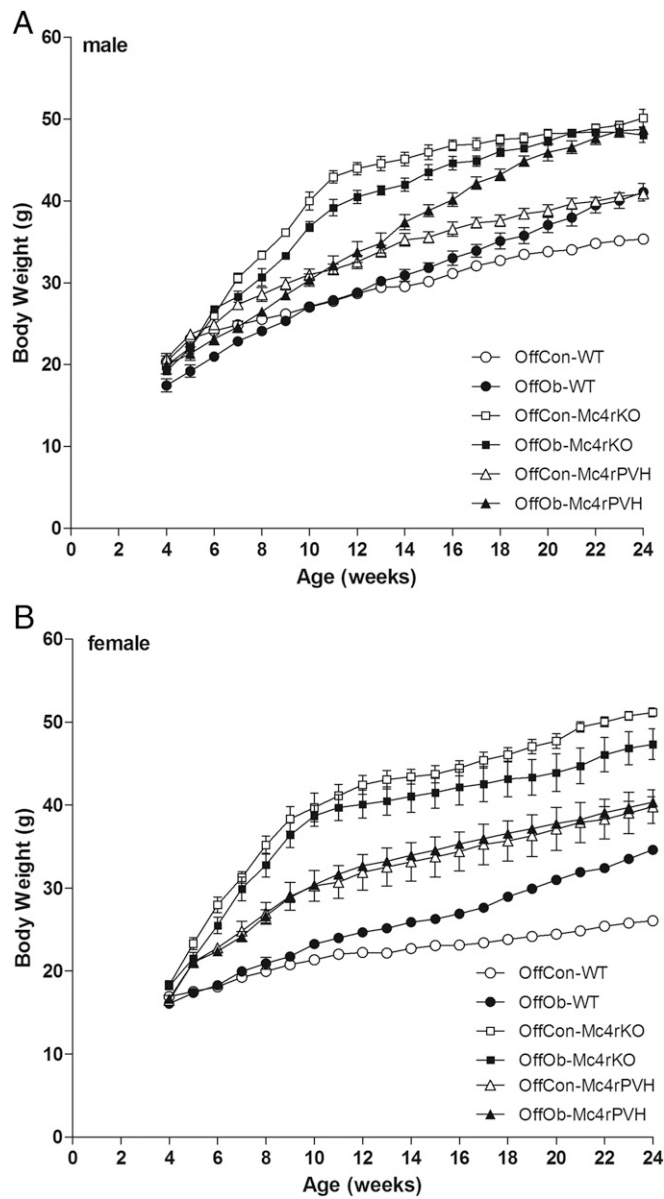
Fig. S4. Growth curves of male (*A*) and female (*B*) OffCon- and OffOb-WT, -Mc4rKO, and -Mc4rPVH mice. Data are expressed as the weekly average per group (*n* = 5–8; mean ± SEM). Male and female OffOb-WT mice demonstrated increased growth vs. OffCon-WT mice ($P < 0.001$, repeated measures ANOVA followed by Tukey post hoc test), and male OffOb-Mc4rPVH mice showed increased growth compared with OffCon-Mc4rPVH mice ($P = 0.008$, repeated measures ANOVA followed by Tukey post hoc test).
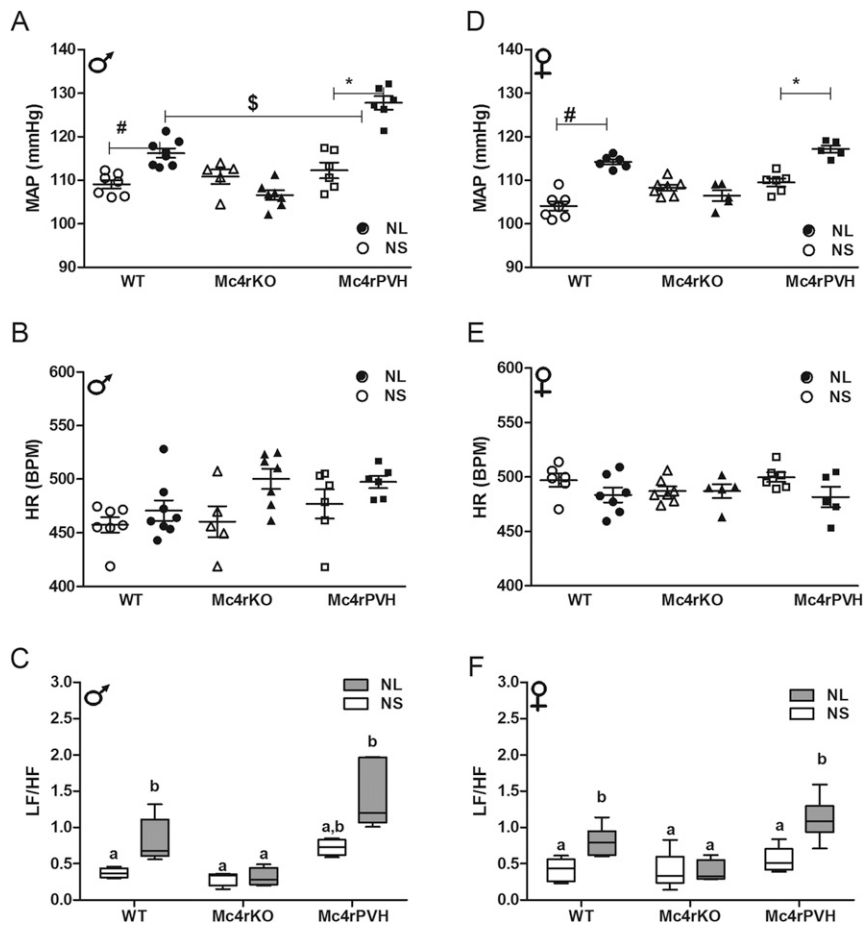
Fig. S5. Mc4r deletion blunts the MAP in NL mice, whereas Mc4rPVH re-expression restores the hypertension. Data in each panel were collected as the average 24-h recordings from 6-mo-old male and female NL (black)- and NS (white)-WT, -Mc4rKO, and -Mc4rPVH mice. MAP (*A* and *D*), HR (*B* and *E*), and LF/HF ratio (*C* and *F*; LF, 0.04–0.15; HF, 0.15–0.40) are shown. *$P < 0.001$ and [#]$P < 0.05$ vs. NS, [$]$P < 0.05$ vs. NL-WT using the Student *t* test (n = 6–8 per group; mean ± SEM). Means not sharing the same letter are significantly different from each other ($P < 0.05$) by generalized least squares (GLS) regression analysis.
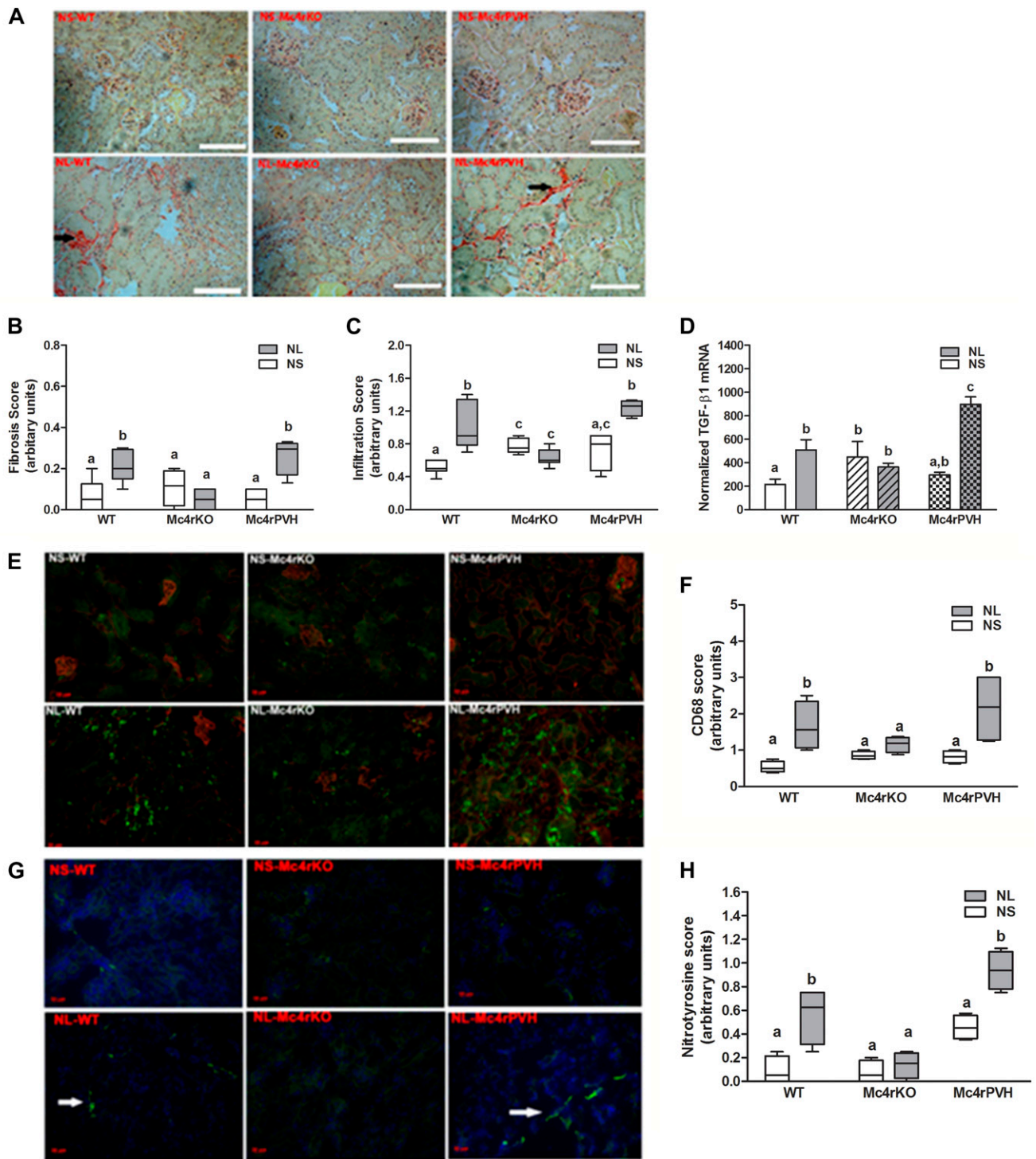
Fig. S6. Representative images of male kidney histology. Note the dense collagen staining (*A*; Picro-Sirus Red) in NL-WT and NL-Mc4rPVH mice corresponding to the male renal expression of fibrotic marker TGF-β1 mRNA (*D*; mean ± SEM; *n* = 4–8) and increased immunoreactivity for CD68 (*E*; AbD Serotec Green) and nitrotyrosine (*G*; Alexa Fluor 488 Green). (Scale bars: *A*, 100 μm; *E* and *G*, 20 μm.) Histological scores for fibrosis (*B*) and infiltration (*C*) from periodic acid–Schiff staining CD68 (*F*, macrophage scavenger) and nitrotyrosine (*H*, oxidative stress marker) immunofluorescence in NS- and NL-WT, -Mc4rKO, and -Mc4rPVH mice. Data are presented as mean ± SEM (*n* = 4–6). Levels were scored as follows: 0, complete absence of immunoreactivity; 1, weak intensity; 2, intermediate intensity; and 3, high intensity. The evaluation was conducted by an investigator blinded to the experimental groups. Means not sharing the same letter are significantly different from each other (*P* < 0.05) by generalized least squares (GLS) regression analysis. Data for females were similar.
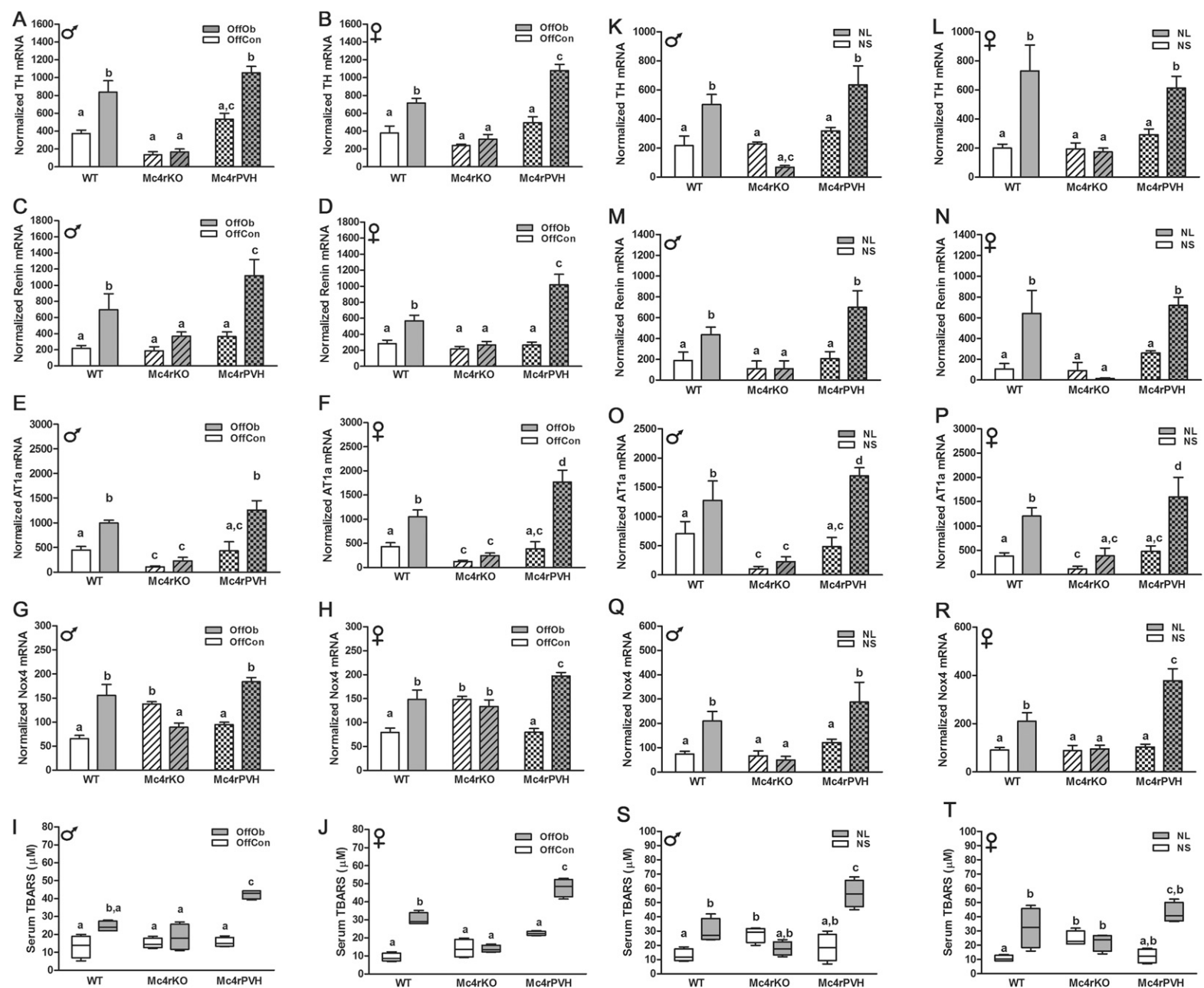
Fig. S7. Enhanced RSNA, RAS, and oxidative stress in OffOb and NL male and female mice. Cortical mRNA expression of TH (*A*, *B*, *K*, and *L*), renin (*C*, *D*, *M*, and *N*), AT1a (*E*, *F*, *O*, and *P*), and Nox-4 (*G*, *H*, *Q*, and *R*; NAPDH oxidase) (*n* = 5–8) and serum TBARS (micromolar) concentration (*I*, *J*, *S*, and *T*) (*n* = 5) in OffOb-WT, -Mc4rKO, and -Mc4rPVH mice and in NL-WT, -Mc4rKO, and -Mc4rPVH mice. Data are presented as the average concentration or normalized value to the GeNorm program values of β-actin and TATAbox. Means not sharing the same letter are significantly different from each other (*P* < 0.05) by generalized least squares (GLS) regression analysis.

Table S1. Number of mice in the study

Experimental condition	Mice, n		
	loxTBMc4r	Sim-1Cre,loxTBMc4r	C57Bl6/J
Maternal diet-induced obesity (n = dams)			
Chow diet (control)	22	18	X
High palatable obesogenic diet (obese)	8	10	X
Neonatal leptin treatment (n = pups)			
NS	9	10	X
NL	9	10	X
Neonatal leptin profiling (n = dams)			
High palatable diet	11	6	3
Chow diet	16	11	3

The number of mothers in each experimental condition used to produce pups in this study is shown with average litter size, prepregnancy weight, and sex. Values are mean ± SD using the Student t test. X, none.

Table S2. Maternal and pup data

Parameters	Mice, n		
	Obese	Control	P value
Prepregnancy weight, g	35.1 ± 2.0	25.4 ± 0.2	$P < 0.001$
Average litter size	7.1 ± 0.8	7.5 ± 0.3	NS
Sex, % female	51	49	NS

The number of mothers in each experimental condition used to produce pups in this study is shown with average litter size, prepregnancy weight, and sex. Values are mean ± SD using the Student t test. NS, nonsignificant.

Table S3. Metabolic characteristics and serum analysis from maternal diet-induced obesity model

Parameters	WT		Mc4rKO		Mc4rPVH	
	OffCon	OffOb	OffCon	OffOb	OffCon	OffOb
Male						
BW, g	36.5 ± 3.4[a]	40.4 ± 3.0[a]	47.8 ± 4.1[b]	51.2 ± 3.6[b]	40.7 ± 2.4[a]	51.4 ± 1.5[b]
WAT, g	0.49 ± 0.15[a]	1.60 ± 0.31[b]	2.66 ± 0.32[c]	2.27 ± 0.31[c]	1.34 ± 0.34[d]	1.96 ± 0.08[c,e]
Muscle, mg	202 ± 12[a]	288 ± 22[b]	270 ± 17[c]	274 ± 17[c]	201 ± 15[a]	216 ± 17[a]
24h-FI, g	1.15 ± 0.35[a]	2.93 ± 0.78[b]	2.31 ± 0.60[b]	3.63 ± 0.57[b]	3.51 ± 0.12[b]	3.56 ± 1.22[b]
24h-EE, H+ kcal/h/kg	12.4 ± 0.7[a]	10.6 ± 0.5[b]	9.8 ± 1.2[b]	10.6 ± 0.4[b]	10.8 ± 0.5[b]	12.5 ± 0.5[a]
Insulin, ng/ml	0.8 ± 0.1[a]	8.7 ± 2.6[b]	10.8 ± 3.8[b]	9.3 ± 3.7[b]	7.5 ± 1.1[b]	9.3 ± 0.7[b]
Leptin	4.6 ± 0.9[a]	11.4 ± 2.3[b]	19.2 ± 2.1[c]	19.7 ± 5.9[c]	13.6 ± 1.3[b]	25.3 ± 1.8[d]
Female						
BW, g	26.9 ± 2.9[a]	35.1 ± 4.3[a]	53.4 ± 2.0[b]	47.9 ± 2.2[b]	42.0 ± 1.7[b]	42.3 ± 3.8[b]
WAT, g	0.34 ± 0.12[a]	1.11 ± 0.22[b]	2.59 ± 0.73[c]	2.29 ± 0.82[c]	0.89 ± 0.14[a]	1.84 ± 0.70[b,d]
Muscle, mg	139 ± 10[a]	162 ± 12[b]	214 ± 16[c]	222 ± 13[c]	185 ± 12[b]	180 ± 17[b]
24h-FI, g	0.85 ± 0.35[a]	2.46 ± 0.35[b]	3.02 ± 0.79[b]	3.17 ± 0.87[b]	2.55 ± 0.43[b]	2.79 ± 1.10[b]
24h-EE, H+ kcal/h/kg	13.0 ± 0.6[a]	10.2 ± 0.7[b]	10.4 ± 0.2[b]	10.0 ± 0.8[b]	10.7 ± 1.3[b]	11.1 ± 1.0[b]
Insulin, ng/ml	1.0 ± 0.4[a]	6.0 ± 1.7[b]	8.0 ± 1.9[b]	11.0 ± 2.1[c]	6.7 ± 1.5[b]	10.1 ± 1.2[b,c]
Leptin, pg/ml	3.9 ± 1.6[a]	15.6 ± 3.1[b]	16.7 ± 1.0[b]	17.5 ± 1.3[b]	15.3 ± 1.6[b]	24.2 ± 0.7[c]

Different alphabetical labels indicate statistical significant difference ($P < 0.05$), using generalized least squares regression analysis. Values are mean ± SD (n = 5–8 per group). Muscle, tibialis anterior; WAT, white adipose tissue.

Table S4.   Metabolic characteristics and serum analysis from neonatal leptin model

Parameters	WT		Mc4rKO		Mc4rPVH	
	NS	NL	NS	NL	NS	NL
Male						
BW, g	33.4 ± 0.5[a]	39.1 ± 0.3[b]	53.3 ± 3.6[c]	47.8 ± 2.4[c]	40.6 ± 1.8[b]	43.5 ± 2.3[b]
WAT, g	0.46 ± 0.08[a]	0.71 ± 0.12[b]	1.65 ± 0.34[c]	1.16 ± 0.42[c]	0.62 ± 0.17[b]	1.11 ± 0.21[c]
24h-FI, g	2.39 ± 0.22[a]	3.46 ± 0.41[b]	6.15 ± 0.56[c]	4.79 ± 0.52[c]	3.32 ± 0.85[a]	4.82 ± 0.72[b]
24h-EE, H+ kcal/h/kg	11.6 ± 1.1[a]	12.1 ± 0.7[a]	10.2 ± 1.15[a]	9.76 ± 0.30[b]	9.71 ± 0.60[b]	9.64 ± 0.63[b]
Insulin, ng/ml	2.1 ± 0.2[a]	3.4 ± 0.8[b]	11.7 ± 1.1[c]	9.1 ± 3.1[c]	8.2 ± 2.9[c]	12.6 ± 2.1[c]
Leptin, pg/ml	3.4 ± 0.7[a]	14.2 ± 1.0[b]	14.6 ± 3.3[b]	18.3 ± 1.6[c]	14.6 ± 1.7[b]	22.0 ± 1.5[c]
Female						
BW, g	28.6 ± 1.7[a]	32.8 ± 3.5[a]	52.9 ± 4.6[b]	48.1 ± 0.7[b]	38.7 ± 7.9[b]	41.9 ± 3.8[b]
WAT, g	0.61 ± 0.08[a]	0.92 ± 0.04[b]	1.62 ± 0.35[c]	1.83 ± 0.02[c]	0.75 ± 0.17[a]	1.30 ± 0.27[b,c]
24h-FI, g	1.42 ± 0.26[a]	3.01 ± 0.47[b]	4.94 ± 0.58[b]	4.68 ± 0.53[b]	1.53 ± 0.79[a]	4.82 ± 0.72[b]
24h-EE, H+ kcal/h/kg	12.3 ± 1.3[a]	12.8 ± 0.9[a]	9.74 ± 0.39[b]	9.96 ± 1.71[b]	10.3 ± 1.7[b]	9.92 ± 0.46[b]
Insulin, ng/ml	2.7 ± 1.5[a]	2.5 ± 0.9[a]	10.8 ± 3.8[b]	10.8 ± 2.0[b]	7.3 ± 2.1[b]	11.0 ± 2.1[b]
Leptin, pg/ml	3.1 ± 1.1[a]	13.5 ± 7.5[b]	16.3 ± 5.5[b]	22.4 ± 1.9[b]	18.0 ± 3.0[b]	20.9 ± 1.9[b]

Different alphabetical labels indicate statistical significant difference ($P < 0.05$), using generalized least squares regression analysis. Values are mean ± SD (n = 5–8 per group).